

Microenvironment Modulation of Metal–Organic Frameworks (MOFs) for Coordination Olefin Oligomerization and (co)Polymerization

Chuan-Lei Zhang,* Tao Zhou, Yong-Qing Li,* Xin Lu, Ye-Bin Guan, Yu-Cai Cao,* and Gui-Ping Cao*

The majority of commercial polyolefins are produced by coordination polymerization using early or late transition metal catalysts. Molecular catalysts containing these transition metals (Ti, Zr, Cr, Ni, and Fe, etc.) are loaded on supports for controlled polymerization behavior and polymer morphology in slurry or gas phase processes. Within the last few years, metal–organic frameworks (MOFs), a class of unique porous crystalline materials constructed from metal ions/clusters and organic ligands, have been designed and utilized as excellent supports for heterogeneous polymerization catalysis whose high density and uniform distribution of active sites would benefit the modulations of molecular weight distributions of high-performance olefin oligomers and (co)polymers. Impressive efforts have been made to modulate the microenvironment surrounding the active centers at the atomic level for improved activities of MOFs-based catalysts and controlled selectivity of olefin insertion. This review aims to draw a comprehensive picture of MOFs for coordination olefin oligomerization and (co)polymerization in the past decades with respect to different transition metal active centers, various incorporation sites, and finally microenvironment modulation. In consideration of more efforts are needed to overcome challenges for further industrial and commercial application, a brief outlook is provided.

1. Introduction

Polyolefins are the most widely used synthetic polymers, in which polyethylene as an example was consumed more than 105 million tons worldwide in 2020. Since the pioneering work by Ziegler^[1] and Natta^[2] in the 1950s, polyethylenes and polypropylenes have been produced using coordination polymerizations at low temperatures and low pressures other than radical polymerization,^[3–6] which became a remarkable milestone in the polyolefin industry. Besides, innovated by the seminal work of Kaminsky^[7] in 1975, the application of single-site metallocene catalysts in olefin polymerization unlocked a new era of high-performance polyolefins. Metallocenes (Figure 1A,B) and subsequent nonmetallocenes (Figure 1C,D) have potential advantages over traditional multisite Ziegler–Natta catalysts as polymer properties can be precisely tuned by definite ligand structures.^[8–11] Furthermore, inspired by Brookhart's initial discovery

of late-transition metal catalysts in 1995,^[12] olefin copolymerization with polar monomers can be catalyzed by various nickel or palladium complexes bearing α -diimine (Figure 1E),^[13,14] phosphine-sulphonate (Figure 1F),^[15,16] and bisphosphine monoxide (Figure 1G)^[17,18] ligands, etc.

Considering most of the commercial polymerization proceeds in a heterogeneous system, supported catalysts have the ability to tailor the microstructure of the synthesized macromolecule with controlled chain length, distribution, particle size, and morphology.^[19,20] Several supports have been investigated by researchers in both industry and academia (e.g., MgCl₂ and SiO₂).^[21–24] Thus, the supports, rationally designed by considering technical aspects such as composition, surface area, particle size, particle size distribution, and porosity, are crucial for tailoring polymer properties in the heterogeneous industrial polymerization processes.^[25]

Metal–organic frameworks (MOFs), a class of porous materials constructed by metal ions wrapped with coordination groups to form small structural units and organic ligands with unique properties and well-defined structures, have attracted great interest over the past decades^[26–29] and showed a wide range of applications in chemical engineering, chemistry, and

C.-L. Zhang, T. Zhou, X. Lu, Y.-B. Guan
Anhui Ultra High Molecular Weight Polyethylene Fiber Engineering Research Center
Anhui Province Key Laboratory of Optoelectronic and Magnetism Functional Materials
Key Laboratory of Functional Coordination Compounds of Anhui Higher Education Institutes
Anqing Normal University
Anqing 261433, P. R. China
E-mail: clzhang@nju.edu.cn
Y.-Q. Li, G.-P. Cao
UNILAB
State Key Laboratory of Chemical Engineering
East China University of Science and Technology
Shanghai 200237, P. R. China
E-mail: gpcao@ecust.edu.cn
Y.-Q. Li, Y.-C. Cao
State Key Laboratory of Polyolefins and Catalysis
Shanghai Key Laboratory of Catalysis Technology for Polyolefins
Shanghai Research Institute of Chemical Industry Co., Ltd
Shanghai 200062, P. R. China
E-mail: liyongqing@srici.cn; caoyc@srici.cn

 The ORCID identification number(s) for the author(s) of this article can be found under <https://doi.org/10.1002/smll.202205898>.

DOI: 10.1002/smll.202205898

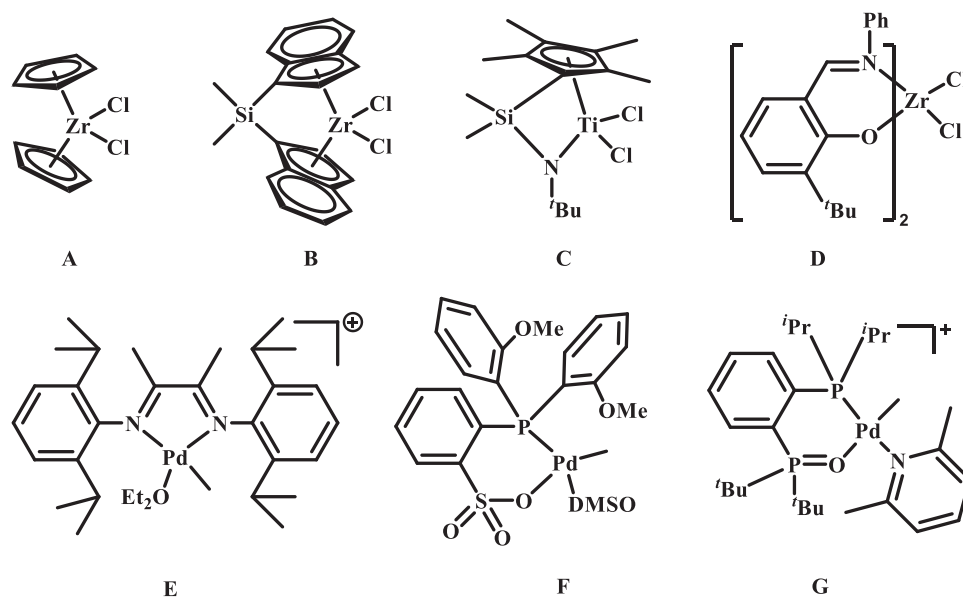


Figure 1. Typical single-site catalysts for olefin polymerization and copolymerization.

materials science,^[30–39] especially in the field of heterogeneous catalysis.^[40–46] Initially, the high orderliness of MOFs facilitate the preparation of single-site supported catalysts, which can be accurately characterized by single crystal X-ray diffraction, and contribute to establish the structure–activity relationship. Besides, MOFs possess numerous active sites separated from each other, which offers opportunities for sufficient coordination between active center and monomer.^[47–49] Moreover, for MOFs that lose catalytic activity due to coordination saturation, the active sites can be constructed by post modification.

MOFs have been first demonstrated as supports for olefin polymerization by Wolczanski et al. in 2001.^[53] In 2009, neodymium-based MOFs as polymerization precatalysts for

isoprene were reported by Visseaux et al.^[54] The application of chromium, nickel, and zirconium-based MOFs in ethylene or propylene oligomerization and polymerization was realized around 2014–2015^[50,55–59] and began to attract wide attention since then.^[60–64] Subsequent research suggested that early (Ti, Zr, Cr, and V)^[58,65–67] and late transition metals (Ni, Co, and Fe)^[68–70] can be incorporated within MOFs in inorganic nodes, organic ligands, and channels (**Figure 2**).

With the purpose of developing novel and industrial available catalysts for precise polyolefin production and searching for new generation of economical and environmental heterogeneous polymerization systems, much effort was dedicated to improving the activities of MOFs-based catalytic systems

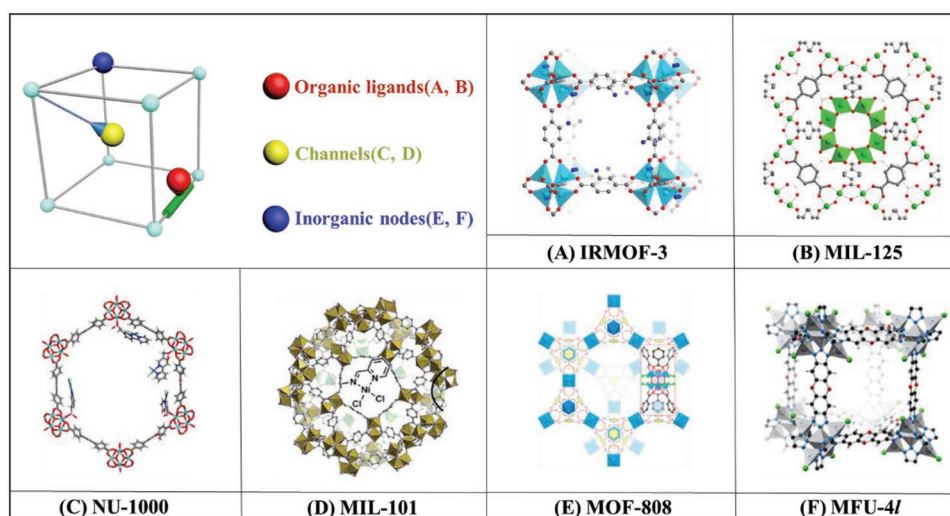


Figure 2. The early and late metal sites in the organic ligands (of A) IRMOF-3 and B) MIL-125), channels (of C) NU-1000 and D) MIL-101) and inorganic nodes (of E) MOF-808 and F) MFU-4l) for ethylene oligomerization and (co)polymerization. C) Reproduced with permission.^[50] Copyright 2015, American Chemical Society. D) Reproduced with permission.^[51] Copyright 2013, American Chemical Society. E) Reproduced with permission.^[52] Copyright 2017, American Chemical Society.

Table 1. The correlation between “elements” and “factors about microenvironment modulation.”

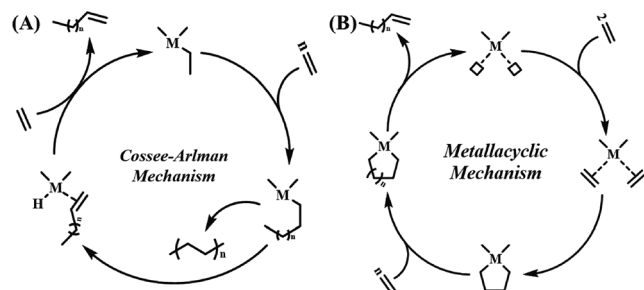
Factors	Electronic effects ¹			Spatial effects ²		
	Metal sites ¹	Coordination atoms ¹	Regulation groups ^{1,2}	Specific surface area ²	Total volume ²	Pore size ²
Inorganic nodes	R ^{a)}	R	R	G ^{b)}	G	G
Organic ligands	R	R	R	G	G	G
Channels	R	R	G	R	R	R

^{a)}“R;” ^{b)}“G” represents relevance and general relevance among them, respectively.

and to controlling the selectivity of olefin insertion. In terms of electronic properties of metal sites, coordinating atoms, and regulation substituents, and spatial effects of specific surface area, total volume and pore size, and regulation groups, the microenvironment^[71] surrounding the active centers has been modulated at the atomic level and proven to influence the coordination oligomerization and (co)polymerization behavior significantly over MOFs-based catalysts. We define inorganic nodes, organic ligands, and channels as “elements,” and metal sites, coordination atoms, regulation groups, specific surface area, total volume, and pore size as “factors.” Their correlations are listed in **Table 1**. With this in mind, this review aims to provide a comprehensive overview of MOFs for coordination olefin oligomerization and (co)polymerization in the past decades with respect to different transition metal active centers, various incorporation sites and finely controlled microenvironment composed by them.

2. Coordination Polymerization Mechanisms

The open coordination sites in most MOFs generally refer to the sites outside the supporting MOF framework that can be obtained by solvent exchange, vacuum activation, methylation, etc., such as the sites occupied by $-Cl$, H_2O , N,N -dimethylformamide (DMF), tetrahydrofuran (THF), etc. In olefin polymerization, the $-Cl$ coordinated sites in MOF can be transformed to open coordination sites through the activation of cocatalysts. After methylation of metal sites, MOF can be used for olefin polymerization to clarify the Cossee–Arlman and Metallacyclic mechanism. The Cossee–Arlman mechanism could explain most of the processes and results of coordination ethylene polymerization or oligomerization within MOFs (**Scheme 1A**).^[72] The metal centers in MOFs are converted to



Scheme 1. A) Cossee–Arlman mechanism and B) metallacyclic mechanism for ethylene oligomerization or polymerization. “M” represents metal centers.

metal-alkyl species with the activation of cocatalysts. Ethylene monomers are inserted into the metal-alkyl bond, leading to the continuous growth of polyethylene chains, or the proceeding of β -H elimination to produce different kinds of oligomers. The metallacyclic mechanism (**Scheme 1B**) was also suggested for oligomerization, in which the olefin monomers were coordinated with vacancies of the metal sites to form metal-cycloalkyl species.^[73] For specific MOFs based catalytic system, the mechanism would be discussed in detail *vide infra*. More detailed mechanisms of olefin polymerization and oligomerization can be found.^[74–76]

3. Construction Methods of Active Sites

MOFs for polyolefin catalysis can be prepared by direct synthesis methods (**Figure 3A**) including sonication exfoliation method^[77] and one-pot solvothermal method.^[59,78] Nonetheless, Postsynthetic modification is essential to embedding active component into the inorganic nodes and organic ligands for MOFs with coordinatively saturated metal sites which are invalid for olefin oligomerization and polymerization.

Postsynthetic modification methods consist of one-pot post-modification, ligand postmodification, ion exchange, solvothermal deposition, and solvent-assisted ligand incorporation. The one-pot postmodification method is the combination of metal–organic complexes containing metal active centers with organic ligands (**Figure 3C**), an example is the formation of metal–organic complexes from 2-pyridinecarboxaldehyde possessing N,O -chelating sites in combination with Ni(II) ions, which then undergo aldehyde amine condensation reactions with the amino groups of $Zn_4O(BDC)_x(ABDC)_{3-x}$ (MixMOFs, BDC = 1,4-benzenedicarboxylate, ABDC = 2-aminobenzene-1,4-dicarboxylate) ligands for the production of MixMOFs-Ni.^[51,55] The ligand postmodification method involves reacting the raw material with the moiety of the organic ligands to form chelate sites, and then binding the target metals with the chelate sites (**Figure 3B**), such as aldehyde amine condensation reactions of 2-pyridinecarboxaldehyde with the amino groups on MIL-125(Ti)-NH₂ (MIL-125(Ti) as $[Ti_8O_8(OH)_4(BDC)_6]$) ligands are performed for the formation of N,N -chelating sites, and then Ni(II) ions are introduced into the chelating sites to prepare MIL-125(Ti)-NH₂-Pyr-Ni (Pyr = 2-pyridinecarboxaldehyde).^[57,79] The ions exchange method is the introduction of the target metals into the inorganic node by metal ions exchange (**Figure 3E**), for example, Zn ions in $Zn_5Cl_4(BTDD)_3$ (MFU-4l, BTDD = 1H-1,2,3-triazolo[4,5-b],[4',5'-i]dibenzo[1,4]dioxin) are replaced with Cr ions to synthesize Cr(II/III)-MFU-4l by

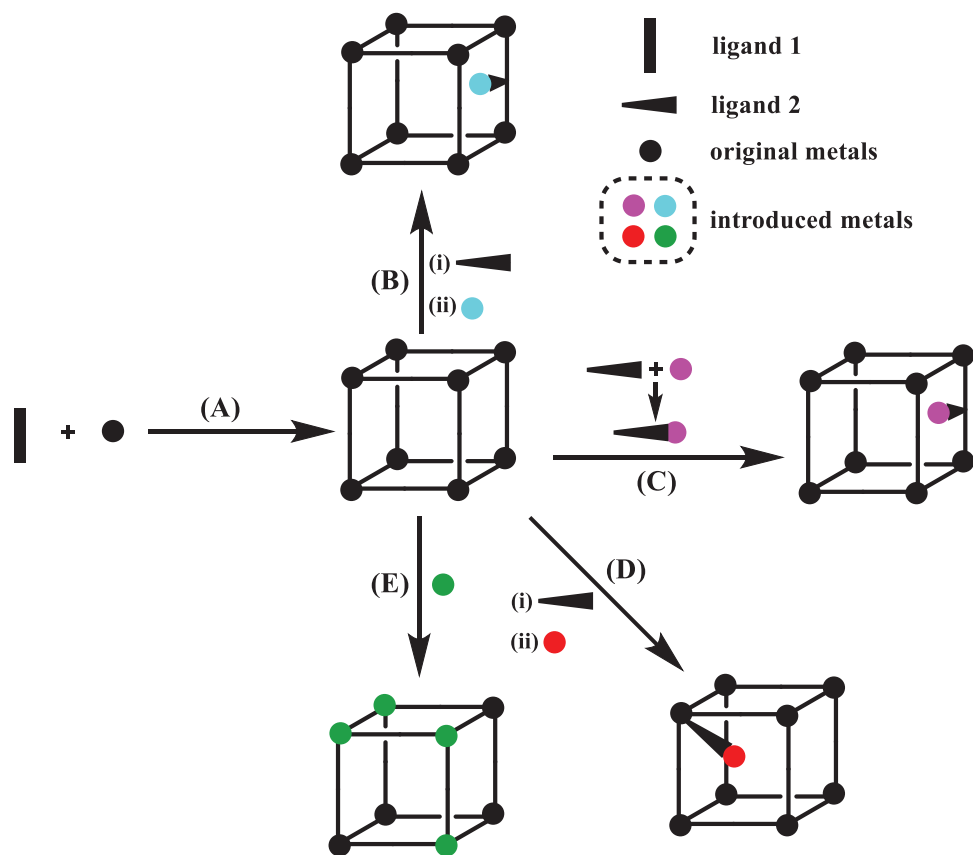


Figure 3. Direct synthesis and postsynthetic modification methods to construct active sites.

immersing MFU-4l in *N,N*-dimethylformamide solutions of CrCl_2 or CrCl_3 .^[66,69,80] The solvent thermal deposition method allows the target metals to be introduced directly into the inorganic nodes (Figure 3E), such that each Cr ion is immobilized in the inorganic nodes by being connected with three oxygen atoms in $[\text{Zr}_6(\mu_3\text{-O})_4(\mu_3\text{-OH})_4]_2(\text{TBAPy})_6$ (NU-1000, TBAPy = 4,4',4'',4'''-(pyrene-1,3,6,8-tetrayl)tetrabenzoate) for the preparation of Cr-solvothermal deposition in MOFs (SIM, solvothermal deposition in MOFs)-NU-1000.^[81,82] Furthermore, active metal centers could be exposed to the channels of MOFs by covalently linking ligands possessing metal active centers with the inorganic nodes (solvent-assisted ligand incorporation method (Figure 3D)), such as ([2,2'-bipyridine]-4-ylmethyl) phosphonic acid monohydrochlorides containing *N,N*-chelating sites are immobilized on the inorganic nodes of NU-1000 via oxy-phosphorus bonds formed by covalent binding, and then Ni(II) ions are introduced into the chelate sites to form NU-1000-bpy(5-methylphosphonate-2,2'-bipyridine)-NiCl₂.^[50]

More detailed direct and postmodification methods for general syntheses of MOFs can be found.^[83,84] In view of these methods, various microenvironment of metal centers within MOFs (Figure 4) for coordination olefin oligomerization and (co)polymerization can be established. To our knowledge, some MOFs possess coordinatively saturated metal sites, such as Ni-UMOFNs, $[\text{cis-Ti}(\mu_{2,7}\text{-OC}_{10}\text{H}_6\text{O})_2\text{py}_2]_n$ and $[\text{cis-Ti}(\mu_{2,7}\text{-OC}_{10}\text{H}_6\text{O})_2(4\text{-picoline})_2(4\text{-picoline})_{0,5}]$, which allow the MOF frameworks to undergo partial metal-oxygen/nitrogen

bond breakage (but not affecting the overall framework) to expose the active sites through high temperature activation before they can be used for olefin polymerization. However, Ni-based MOFs, including Ni/UiO-66($[\text{Zr}_6\text{O}_4(\text{BDC})_6]$), Ni₂(dobdc) and Ni₂(dobpdc) (dobdc = 2,5-dioxido-1,4-benzenedicarboxylate, dobpdc = 4,4-dioxido-[1,1'-biphenyl]-3,3'-dicarboxylate), have original coordinatively unsaturated metal active centers for olefin polymerization without the activation of cocatalysts. The vast majority of MOFs, such as M-MFU-4l (M = Ni, CO, Ti, V), MixMOFs-Ni, ZrCl₂-BTC, etc., can be treated by solvent exchange, vacuum activation, and methylation to remove terminal coordination small molecules and groups (e.g., H₂O, -Cl, tetrahydrofuran (THF), etc.) to complete the activation of metal sites for heterogeneous polymerization reactions.

4. Early Transition Metal-Based MOFs

Early transition metal catalysts, such as Ziegler–Natta catalysts,^[85] metallocene catalysts (Figure 1A,B),^[86] constrained geometry catalysts (Figure 1C),^[87] and FI catalysts (Figure 1D)^[88] etc., were found to exhibit unprecedented activities toward industrial olefin polymerization. The activities of catalytic sites can be exquisitely modulated by designing relevant organic ligands, which can subsequently adjust the morphologies of polymer particles, increase molecular weight (MW), tailor polymer dispersity, and improve mechanical property and

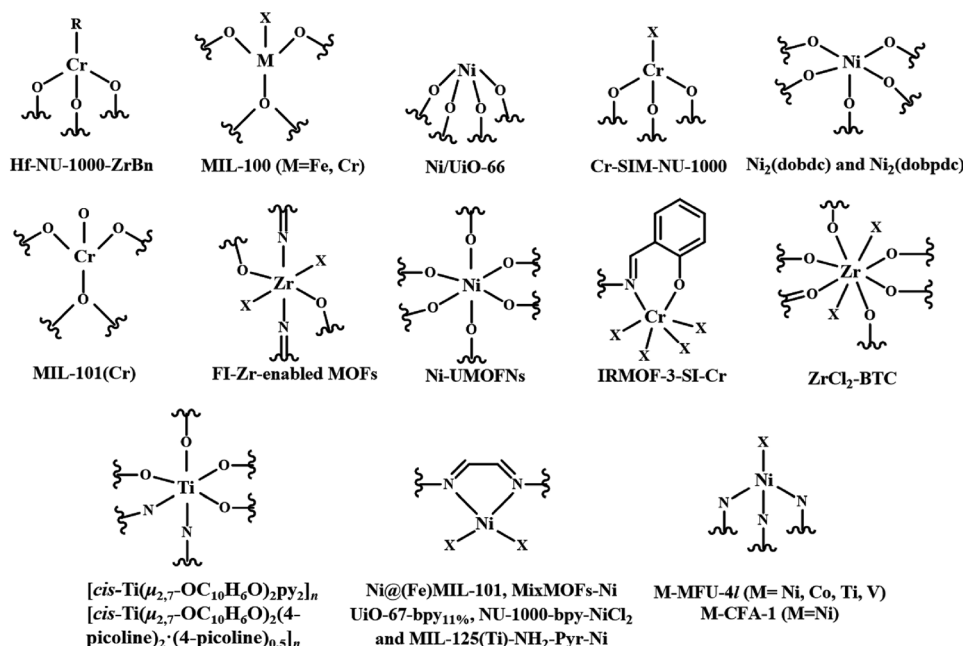


Figure 4. The coordination environment of metal sites in MOFs, “X,” and “R” represent halogen atoms and tetrabenzyl group, respectively.

processing performance of the (co) polymers.^[89–93] Since Wolczanski’s initial work,^[53] Zr, Cr, Ti, and V were introduced into the inorganic nodes and organic ligands in the microenvironment of the framework to construct early transition metal-based MOFs.

4.1. Zirconium-Based MOFs

Zr-based metallocene and nonmetallocene catalysts are widely used with high activity, and Zr-based MOFs are also intensively studied for olefins polymerization. Zr ions have been introduced into the inorganic nodes and channels in the microenvironment of MOFs through postsynthetic modifications and considered to have potential advantage over stereoregularity modulation of polymer chains through the activities of Zr-based MOFs are generally moderate.

4.1.1. Metal Sites in the Inorganic Nodes

Highly electrophilic Zr-based active species (ZrBn, Bn = tetrabenzyl group) were incorporated into the inorganic nodes of Hf-NU-1000 by Farha and coworkers^[58] in 2015 (Figure 5). At room temperature, highly stereoselective polymerization of 1-hexene (isotacticity > 95%) was achieved by the MOFs-based single site and single component catalyst for the first time. Ascribed to different microenvironment between interior and exterior active sites, the obtained poly(1-hexene) showed bimodal distribution (weight average molecular weight (M_w) = 5.3×10^5 in the high MW fraction with dispersity (D) = 1.9 and M_w = 680 in the low molecular weight (MW) fraction with D = 1.2). For the microenvironment modulation of Hf-NU-1000-ZrBn, the activity of Hf-NU-1000-ZrBn catalyzed ethylene polymerization

was low (9.3×10^3 g_{PE} mol_{Zr}⁻¹ h⁻¹) and even lower for the polymerization of 1-hexene (2.4×10^3 g_{PH} mol_{Zr}⁻¹ h⁻¹), which could be attributed to the occurrence of toluene elimination reaction to generate MOFs with no polymerization activity and the spatial restriction effect of microenvironment. It is noteworthy that the MW of the obtained linear polyethylene (PE) with poor solubility and high melting temperature (142 °C) is presumed to be ultrahigh MW level.

Catalytic performance can be improved by adjusting the microenvironment of the active centers. Lin and coworkers^[52] transformed the secondary building units (SBUs) in [Zr₆O₄(OH)₄(BTC)₂(HCOO)₆] (MOF-808, BTC = benzene-1,4-tricarboxylate) into hexanuclear precatalyst for high MW (M_w up to 7.9×10^5) linear polyethylene production in 2017 (Figure 6). For the microenvironment modulation of ZrCl₂-BTC, 30-fold increase of activity along with an eightfold increase of ethylene

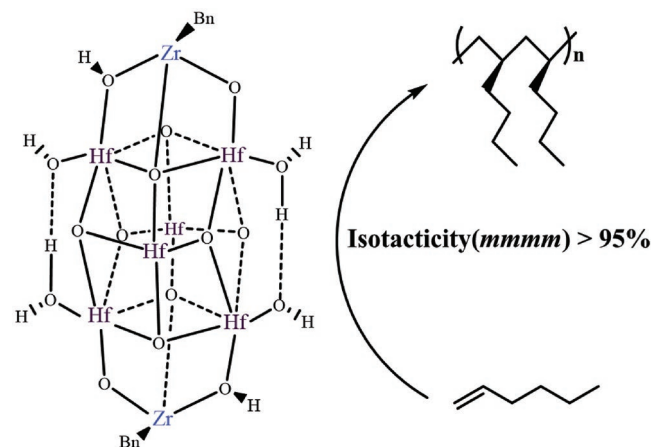


Figure 5. Hf-NU-1000-ZrBn for 1-hexene polymerization.

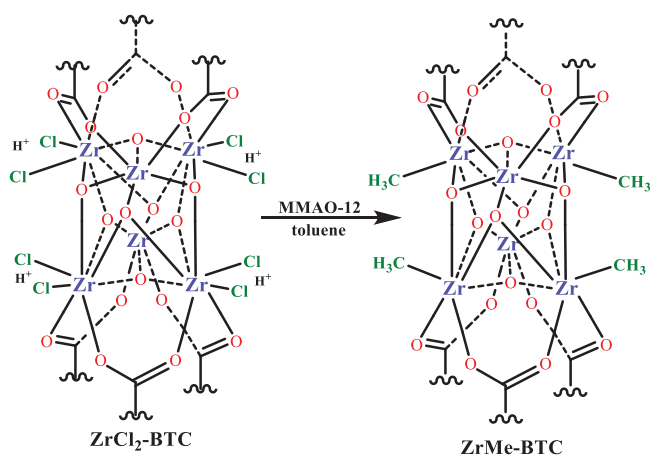


Figure 6. $\text{ZrCl}_2\text{-BTC}$ for ethylene polymerization.

pressure as a result of exposure of more active sites with the activation of MMAO-12 stemmed from polymer-induced fracture of the MOF particles was observed with $\text{ZrCl}_2\text{-BTC}$ (activity up to $6.6 \times 10^5 \text{ g}_{\text{PE}} \text{ mol}_{\text{Zr}}^{-1} \text{ h}^{-1}$ at 100 °C and 55 bar ethylene pressure). Interestingly, it was also observed that the D of polyethylene obtained at low pressure (6.9 bar) depended on the polymerization temperature. Narrow D was generated at $\approx 20\text{--}80$ °C ($D = \approx 2.44\text{--}3.55$), while widened significantly at $\approx 100\text{--}140$ °C ($D = \approx 4.91\text{--}7.79$), which might be attributed to the blocked diffusion of ethylene to the active sites in the microenvironment caused by the solvent-swelling effect of polyethylene chains at high temperature. Besides, site isolation of the MOFs may have been an important factor in the stabilization and long life-time of active sites in the microenvironment. The MOFs still kept its original high activity and crystallinity in 12 h of polymerization at 100 °C, which was confirmed by powder X-ray diffraction (PXRD).

4.1.2. Metal Sites in the Channels

Under the promise of more flexible structure modulation for more diverse microenvironment, FI (bis(phenoxy-imine)) type Zr sites surrounded by bulky phenyl and cyclohexyl substituents installed on the N atoms were introduced into the channels of MOFs (Figure 7, **FI-Ph** and **FI-Cy** (Ph = phenyl, Cy = cyclohexyl)) by Mu and co-workers.^[59] At 50 °C and Al/Zr = 50 (mol mol^{-1}), **FI-Cy** and **FI-Ph** exhibited the highest activity (1.38×10^6 and $3.9 \times 10^5 \text{ g}_{\text{PE}} \text{ mol}_{\text{Zr}}^{-1} \text{ h}^{-1}$, respectively) toward the production of linear polyethylene irregular particles with a diameter of ≈ 1 μm , and the MWs of 1.5×10^5 and 3.6×10^5 were afforded with the corresponding catalyst. For the microenvironment modulation of **FI-Cy** and **FI-Ph**, the catalytic differences of **FI-Cy** and **FI-Ph** might be in part related to the porosity parameters of the MOFs. The Brunauer–Emmett–Teller (BET) specific surface areas are 479 and 230 $\text{m}^2 \text{ g}^{-1}$, and the total volumes are 0.31 and 0.17 $\text{cm}^3 \text{ g}^{-1}$ for **FI-Cy** and **FI-Ph**.

The effective activation of metal centers upon cocatalysts was influenced by the limited environment (microenvironment) in channels, thus bulky MAO activated ethylene polymerization possessed low efficiency. In contrast, activated by triisobutyl

aluminum (Al^iBu_3)/ $\text{Ph}_3\text{CB}(\text{C}_6\text{F}_5)_4$, **FI-Cy** showed smoother release of activity and longer lifetime (3 h) and afforded higher productivity compared to the unsupported parent FI catalyst bis[N-(3-*tert*-butylsaliicyl-dene)cyclohexylamino]zirconium(IV) dichloride which showed fast activity release and deactivation. Chain transfer and $\beta\text{-H}$ elimination effects were also inhibited in channels, while the microenvironment on the surface of MOFs was similar to the unsupported catalyst. Accordingly, bimodal polyethylenes with an $\approx 70\text{--}80\%$ high MW fraction, wide D ($D = \approx 10.1\text{--}14.0$ and $\approx 17.47\text{--}20.9$, respectively) and high MWs ($\approx 1 \times 10^5\text{--}5 \times 10^5$) were produced with **FI-Cy** and **FI-Ph** in contrast to the single site characteristic with the unsupported catalyst ($D = 2.76$, $\text{MW} = 1.5 \times 10^4$).

4.2. Chromium-Based MOFs

In the 1950s, Cr-based heterogeneous olefin polymerization catalysts were developed by Phillips and played a key role in the polyolefin industry.^[94] The properties of polyolefins obtained from multisite Cr-based catalysts might be influenced by the homogeneity of the active components in the microenvironment.^[95,96] Cr-based MOFs could be also used for the production of high MW polyethylene, which are promising catalysts for the slurry phase process.

4.2.1. Metal Sites in the Inorganic Nodes

The amount of cocatalysts obviously affects the properties of the metal sites in the microenvironment and thus has great impact on the catalytic activity and the MW of polymerization products. Cr-SIM-NU-1000 with an average pore size close to 3 nm prepared by thermally depositing Cr(III) ions (Figure 8) in the inorganic nodes of NU-1000 was reported by Farha et al.^[81,82] For the microenvironment modulation of Cr-SIM-NU-1000, diethylaluminum chloride (AlEt_2Cl)-treated Cr-SIM-NU-1000 (Al/Cr = 3/1) was active ($1.68 \times 10^3 \text{ g}_{\text{oligomers}} \text{ mol}_{\text{Cr}}^{-1} \text{ h}^{-1}$) for $\text{C}_8\text{--C}_{18}$ formation with moderate selectivity (79%) at room temperature and rather low ethylene pressure (1 bar). However, with the molar ratio of Al/Cr increased to 287/1, AlEt_2Cl -treated Cr-SIM-NU-1000 exhibited moderate activity ($1.3 \times 10^5 \text{ g}_{\text{PE}} \text{ mol}_{\text{Cr}}^{-1} \text{ h}^{-1}$) for the production of crystalline linear polyethylene ($M_w = 9.2 \times 10^5$) with narrow D ($D = 2$) at 25 °C and 40 bar ethylene pressure. In contrast to $\text{ZrCl}_2\text{-BTC}$,^[52] Cr-SIM-NU-1000 catalyzed ethylene polymerization had a tendency to a linear dependence of turnover frequency on ethylene pressure, which reveals the structural stability of the latter. Given the essential activation of AlEt_2Cl , the obtained linear ethylene and the lack of olefinic terminal, Cossee–Arlman mechanism (Scheme 1) was proposed for Cr-SIM-NU-1000 catalyzed ethylene polymerization.

The vacuum activation temperature influences the specific surface area and pore volume of MOFs, thus affecting the formation of active sites and the subsequent coordination-insertion of ethylene with metal sites. A series of $\text{Cr}_3\text{F}(\text{H}_2\text{O})_3 \text{O}[\text{C}_6\text{H}_3(\text{CO}_2)_3]_2 \cdot 28\text{H}_2\text{O}$ (MIL-100(Cr)-*t*), where *t* represents the evacuated temperatures, was synthesized by Zhang et al.^[78] for ethylene oligomerization, and exhibited moderate catalytic

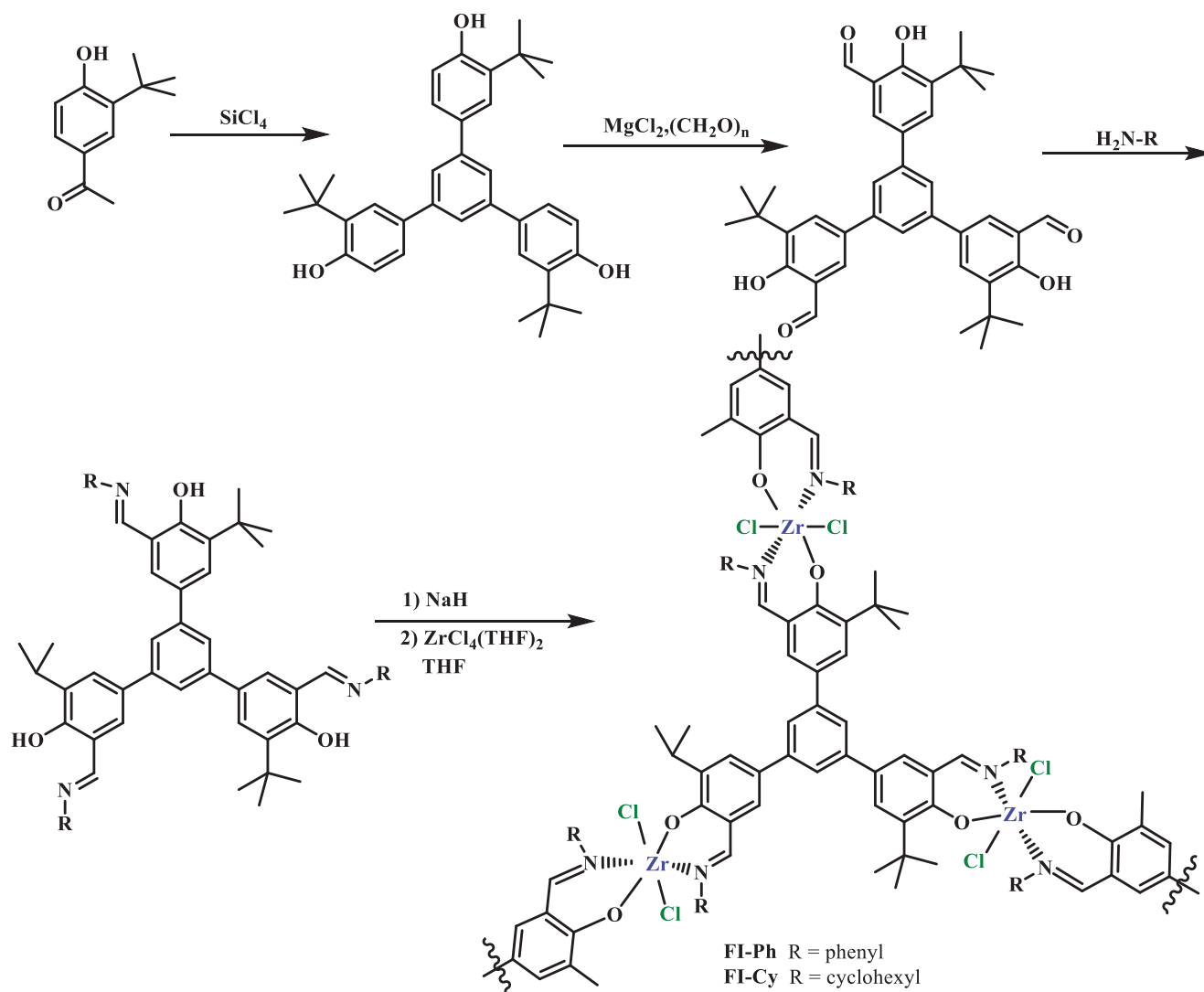


Figure 7. Synthesis of FI-Zr-MOFs (FI-Ph and FI-Cy).

activity ($\approx 3.44 \times 10^5$ – 9.27×10^5 $\text{g}_{\text{oligomers}} \text{mol}_{\text{Cr}}^{-1} \text{h}^{-1}$) and selectivity (≈ 80 – 90%) for the overall product of ethylene tetramerization and pentamerization at 10°C and 10 bar ethylene pressure. For the microenvironment modulation of MIL-100(Cr), MIL-

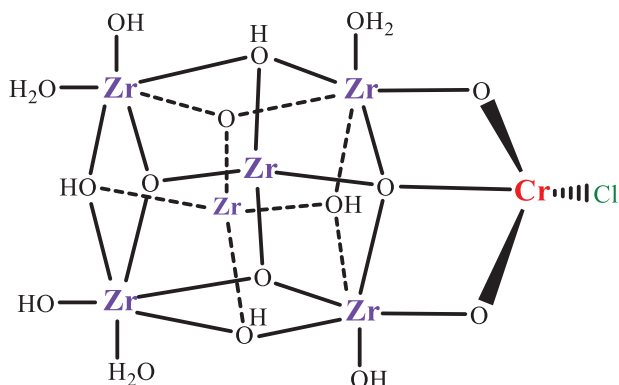


Figure 8. The coordination environment of Cr(III) sites in Cr-SIM-NU-1000.

100(Cr)-250 exhibited the highest specific surface area ($2348 \text{ m}^2 \text{ g}^{-1}$) and pore volume ($1.29 \text{ cm}^3 \text{ g}^{-1}$), which facilitated the sufficient contact of ethylene with the active centers, resulting in the highest activity (9.27×10^5 $\text{g}_{\text{oligomers}} \text{mol}_{\text{Cr}}^{-1} \text{h}^{-1}$) (Table 2). Single metal and dimetallic active sites regarding the evacuation process of MOFs is presumed to be involved in the metal-cyclic mechanism (Scheme 2) as the pore size (2.5–2.9 nm) of MIL-100(Cr) is larger than that of the oligomerization products (1.4 nm). The selective formation of C_4 , C_6 , C_8 , and C_{10} through different metallacycle on single Cr(III) sites or cooperative reductive elimination of two metallacycles on dimetallic Cr(III) sites is depended on different evacuation conditions. Polyethylene by-product resulted from Cr(II) active sites in MIL-100(Cr)-250 catalyzed oligomerization was characterized by various techniques. It was observed that the obtained linear polyethylene had nanofibrous morphology, ultrahigh MW (M_w up to 1.2×10^7) and broad D ($D = 24$).

The activation of the cocatalysts affects the pore size, shape, and pore volume, which has an impact on the exposure opportunity and activity of the active sites. Weckhuysen et al.^[97]

Table 2. Porosity parameters and ethylene oligomerization performance of MIL-100(Cr)-*t*.

MIL-100(Cr)- <i>t</i> ^{a)}	S_{BET} [m ² g ⁻¹]	S_{Langmuir} [m ² g ⁻¹]	Pore volume [cm ³ g ⁻¹]	Activity ^{b)}	Selectivity [%]			
					C ₄	C ₆	C ₈	C ₁₀
150	1905	2686	1.04	5.13	0.27	26.36	69.15	4.22
200	1954	2754	1.08	7.07	7.03	0.02	52.26	40.69
250	2348	3323	1.29	9.27	1.07	18.89	40.14	39.18
300	1930	2725	1.07	3.94	2.18	2.81	38.62	56.39
350	1917	2721	1.10	3.44	—	0.98	59.44	39.58

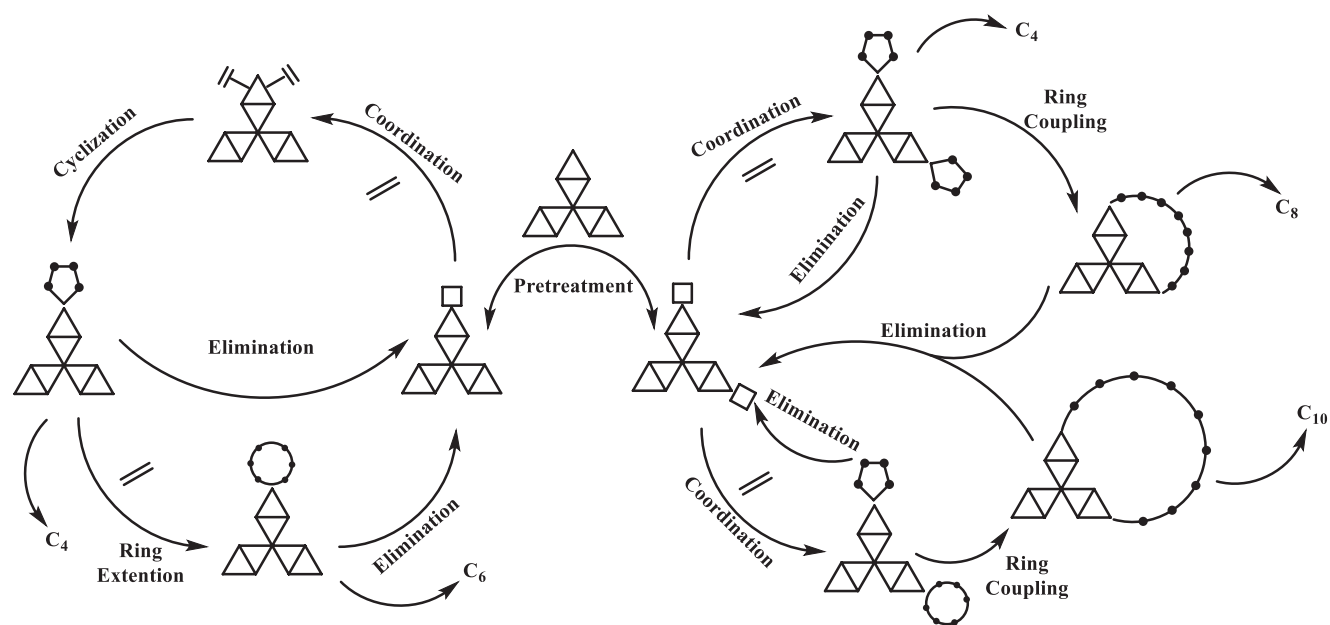
^{a)} AlEt₂Cl as cocatalyst [Cr] = 5 × 10⁻⁵ mol L⁻¹, n(Al)/n(Cr) = 500, P = 10 bar, *t* = 1 h, T = 10 °C; ^{b)} Unit of 10⁵ g_{oligomers} mol_{Cr}⁻¹ h⁻¹.

performed a series of different pretreatments of MIL-100(Cr) and Cr₃F(H₂O)₂O[(O₂C)C₆H₄(CO₂)₃·25H₂O (MIL-101(Cr)) for ethylene polymerization (Figure 9). Activated by Et₂AlCl, MIL-100(Cr) did not undergo any significant structural changes, which resulted in insufficient contact of the active centers with the monomer in the microenvironment, and showed extremely low activity (2.1 g_{PE} mol_{Cr}⁻¹ h⁻¹) for ethylene polymerization at 25 °C and 10 bar ethylene pressure. In contrast, the active component was leached from MIL-101(Cr) for the production of irregular polyethylene fibers with the activation of diethyl aluminum chloride (Et₂AlCl), which was explained by the inability of active species to control the polymer performances after leaving the microenvironment within MOFs.

For the microenvironment modulation of MIL-101(Cr), this MOF partially collapsed to form porous structure with the activation of Et₂AlCl was active (1.54 × 10⁴ g_{PE} mol_{Cr}⁻¹ h⁻¹) for the production of polyethylene with *M_w* of 1.1 × 10⁴ at the expense of structural integrity. The obtained polyethylene was micrometer-sized beads with regular structure. Therefore, MIL-101(Cr)

could be used as good porous template for the production of polymers with specific morphology and stereoregularity, thereby control the processing and physical properties of the product.

Earlier work in this field involving heterogeneous polymerization catalysis with Cr-based MOFs had shown the potential and development prospects of MOF-supported molecular Cr catalysts for ethylene polymerization and ethylene-propylene copolymerization. Dincă and co-workers^[66] prepared Cr(II)-MFU-4l and Cr(III)-MFU-4l by treating MFU-4l with CrCl₃(THF)₂(H₂O) and CrCl₂ solutions, respectively. At 40 bar ethylene pressure and 23 °C, Cr(II)-MFU-4l exhibited moderate activity (1.3 × 10⁵ g_{PE} mol_{Cr}⁻¹ h⁻¹) for polyethylene formation, and high MW polyethylene (*M_w* up to 7 × 10⁵) with broad D (*D* = 7) was obtained. Cr(III)-MFU-4l was active (9.6 × 10⁴ g_{PE} mol_{Cr}⁻¹ h⁻¹) for the slurry-phase production of high MW polyethylene (*M_w* = 5 × 10⁵) with broad D (*D* = 5). On the other hand, activated by methylaluminoxane (MAO), Cr(III)-MFU-4l was able to copolymerize ethylene with propylene (incorporation ratios were ≈1.5–2.5%).



Scheme 2. The metallacyclic mechanism for ethylene oligomerization processes on MIL-100(Cr).

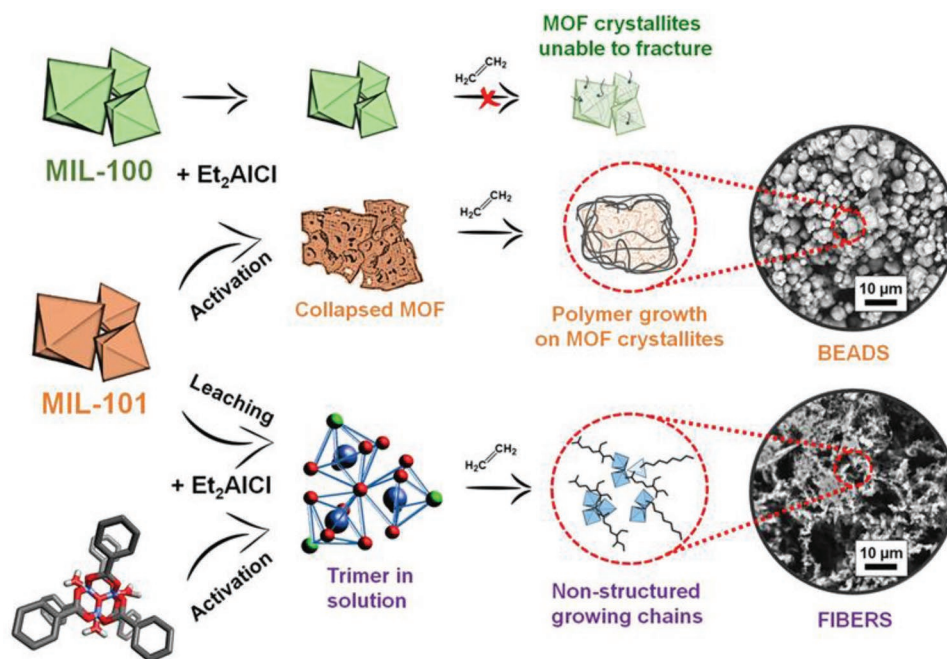


Figure 9. MIL-100(Cr) and MIL-101(Cr) for ethylene polymerization after a series of different pretreatments.

The change of polymerization environment also affects the metal-ethylene coordination and subsequent polyethylene chains growth in the microenvironment. Cr(III)-MFU-4l could be also applied in the gas phase process for ethylene polymerization. Dincă and coworkers^[67] synthesized Cr(III)-MFU-4l by ion exchange with MFU-4l (**Figure 10**). At room temperature and 40 bar ethylene pressure, trimethyl aluminum (AlMe_3)-treated Cr(III)-MFU-4l was more active ($1.45 \times 10^6 \text{ g}_{\text{PE}} \text{ mol}_{\text{Cr}}^{-1} \text{ h}^{-1}$) in gas-phase polymerization than the slurry-phase process (e.g., Cr(III)-MFU-4l of $1.5 \times 10^5 \text{ g}_{\text{PE}} \text{ mol}_{\text{Cr}}^{-1} \text{ h}^{-1}$), and high MW polyethylene (M_w close to 4×10^5) with narrow D ($D = 1.36$) was generated. Compared to the slurry-phase environment, the metal sites in the microenvironment of Cr(III)-MFU-4l are more easily coordinated with ethylene in the gas-phase environment, thus facilitating subsequent chain growth to obtain high MW polyethylene. In addition, single-site Cr(III)-MFU-4l is highly suitable for gas-phase ethylene polymerization since the obtained granular form polyethylene facilitates industrial processing.

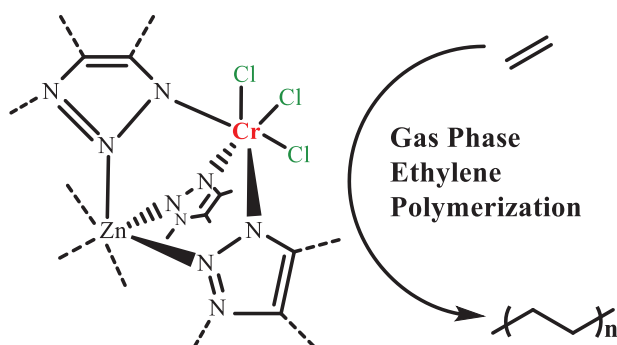


Figure 10. Cr(III)-MFU-4l for the gas-phase ethylene polymerization.

4.2.2. Metal Sites in the Organic Ligands

Recently, Jie and co-workers^[57] installed Cr(III) ions on the organic ligands of IRMOF-3-SI (IRMOF-3 = $[\text{Zn}_4\text{O}(\text{ATA})_3]$, ATA = aminoterephthalic acid) and synthesized IRMOF-3-SI-Cr by post-synthetic modification (**Figure 11**). Methylaluminoxane (MAO), trimethylaluminium (TMA), triethylaluminium (TEA), and triisobutylaluminium (TIBA) were used to activate MOFs for ethylene polymerization, respectively (**Table 3**). Activated by TIBA at 50 °C, IRMOF-3-SI-Cr showed the highest activity ($8.4 \times 10^4 \text{ g}_{\text{PE}} \text{ mol}_{\text{Cr}}^{-1} \text{ h}^{-1}$) and afforded high MW polyethylene ($M_w = 4 \times 10^5$) with broad D ($D = 13.5$). The microenvironment surrounding active Cr(III) sites closely related with activity in IRMOF-3-SI-Cr and the performance of polyethylene are dramatically influenced by both the loading and type of cocatalysts. For the microenvironment modulation of IRMOF-3-SI-Cr, Cr-Cl species are activated by cocatalysts (e.g., TMA, TEA, and TIBA) for the formation of Cr-alkyl species. The larger space volume of isobutyl than methyl and ethyl makes Cr-isobutyl species more difficult to be present under ethylene stimulation, which results in easier generation of coordinatively unsaturated Cr active centers in the microenvironment for the coordination of metal sites with ethylene and subsequent polymer chains growth.

4.3. Vanadium and Titanium-Based MOFs

Activated by MAO, 1D $[\text{cis-Ti}(\mu_{2,7}\text{-OC}_{10}\text{H}_6\text{O})_2\text{py}_2]_n$ was active ($1 \times 10^3 \text{ g}_{\text{PP}} \text{ mol}_{\text{Ti}}^{-1} \text{ h}^{-1}$) for propylene polymerization to produce polypropylene ($M_w = 2.7 \times 10^4$) with broad D ($D = 8$) at 23 °C and 5 bar propylene pressure,^[53] and also active for ethylene polymerization ($2.8 \times 10^4 \text{ g}_{\text{PE}} \text{ mol}_{\text{Ti}}^{-1} \text{ h}^{-1}$). Similarly, 2D $[\text{cis-Ti}(\mu_{2,7}\text{-OC}_{10}\text{H}_6\text{O})_2(4\text{-picoline})_2 \cdot (4\text{-picoline})_{0.5}]_n$ showed moderate activity ($1.2 \times 10^4 \text{ g}_{\text{PE}} \text{ mol}_{\text{Ti}}^{-1} \text{ h}^{-1}$) for ethylene

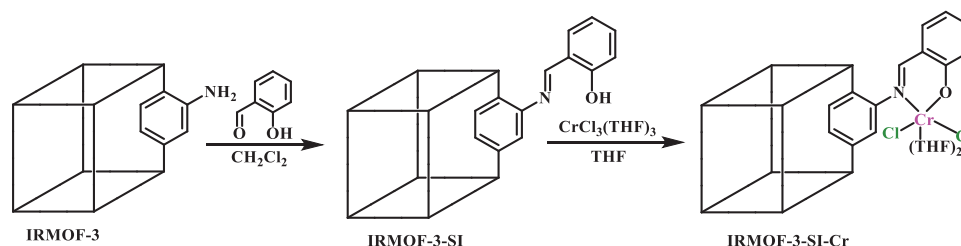


Figure 11. Preparation of IRMOF-3-SI-Cr by postsynthetic modification of IRMOF-3.

polymerization and low active for polypropylene formation ($500 \text{ g}_{\text{PP}} \text{ mol}_{\text{Ti}}^{-1} \text{ h}^{-1}$). Although metal sites in these Ti-based MOFs possess the almost same coordination environment, monomers are more readily accessible to the metal sites in the 1D catalyst with beneficial microenvironment than the 2D one (Figure 4K), which leads to higher activity of the former for ethylene and propylene polymerization.

Ti and V ions are coordinated with three N atoms in 3D MFU-4l framework. Recently, Dincă and co-workers^[66] have successfully incorporated Ti(III) and Ti(IV) ions into the inorganic nodes by treating MFU-4l with excess $\text{TiCl}_3(\text{THF})_3$ and $\text{TiCl}_4(\text{THF})_2$. In ethylene polymerization, Ti(III)-MFU-4l showed high activity ($4.2 \times 10^5 \text{ g}_{\text{PE}} \text{ mol}_{\text{Ti}}^{-1} \text{ h}^{-1}$) and produced high-density granular polyethylene ($M_w = 9 \times 10^5$) from MFU-4l templates with broad D ($D = 3$) at 40 bar ethylene pressure and 23 °C. The effective coordination of free flowing monomer molecules with catalytic sites in the microenvironment and the uniform growth of polymer chains in MOFs is beneficial for the regulation of polymer morphology.

In ethylene-propylene copolymerization, Ti(III)-MFU-4l and Ti(IV)-MFU-4l produced copolymers with $\approx 3\text{--}8\%$ propylene incorporation ratio and long branched chains, which can improve the melting temperatures of the copolymers (Table 4).

V(II)-MFU-4l and V(IV)-MFU-4l prepared by incorporating V(II) and V(IV) ions into MFU-4l for ethylene and propylene polymerization were initially reported by Dincă and co-workers (Figure 12A).^[65] At 40 bar ethylene pressure and 25 °C, V(IV)-MFU-4l exhibited high activity ($2 \times 10^6 \text{ g}_{\text{PE}} \text{ mol}_{\text{V}}^{-1} \text{ h}^{-1}$), affording high MW polyethylene (M_w up to 2.2×10^6) with broad D ($D = 3.4$) (Figure 12B). Furthermore, activated by MMAO-12, V(II)-MFU-4l was able to produce higher MW polyethylene (M_w up to 2×10^6), although the activity of V(II)-MFU-4l ($1.8 \times 10^5 \text{ g}_{\text{PE}} \text{ mol}_{\text{V}}^{-1} \text{ h}^{-1}$) was lower than that of V(IV)-MFU-4l ($1.4 \times 10^6 \text{ g}_{\text{PE}} \text{ mol}_{\text{V}}^{-1} \text{ h}^{-1}$, $M_w = 1.2 \times 10^6$) at 10 bar ethylene pressure. For the microenvironment modulation of V-MFU-4l, the V(II) sites bind more strongly with $\beta\text{-H}$ than V(IV) sites in the microenvironment of V(II)-MFU-4l and V(IV)-MFU-4l, which makes it more difficult for $\beta\text{-H}$ elimination and polymer chains transfer to occur in V(II)-MFU-4l, resulting in the production of higher MW polyethylene with V(II)-MFU-4l.

Benefiting from highly ordered channels (good microenvironment), V(IV)-MFU-4l was active ($150 \text{ g}_{\text{PP}} \text{ mol}_{\text{V}}^{-1} \text{ h}^{-1}$) for propylene polymerization and produced isotactic polypropylene (PP, $m > 94\%$, m is the mass) with good mechanical and processing performance (Figure 12C). Moreover, V(II)-MFU-4l and V(IV)-MFU-4l showed good stability since they

Table 3. Ethylene polymerization with IRMOF-3-SI-Cr and various cocatalyst.

Entry ^{a)}	Co-cat.	Al/Cr	Activity [$10^4 \text{ g}_{\text{PE}} \text{ mol}_{\text{Cr}}^{-1} \text{ h}^{-1}$]	Number average molecular weight (M_n) ^{b)} [kg mol^{-1}]	D^b	Melting peak (T_m) ^{c)} [°C]
1	MAO	500	1.93	10.0	31.9	134.6
2	MAO	1000	1.82	9.1	30.9	133.6
3	MAO	2000	2.05	7.5	37.3	133.2
4	TMA	60	1.13	14.8	20.2	135.1
5	TMA	300	1.22	9.5	33.2	134.8
6	TEA	30	0	—	—	—
7	TEA	60	3.11	14.0	33.6	135.1
8	TEA	120	3.29	14.3	27.4	134.2
9	TEA	300	3.44	10.3	37.0	134.2
10	TIBA	60	0	—	—	—
11	TIBA	120	3.98	29.5	12.5	135.2
12	TIBA	300	5.91	23.2	16.2	135.4
13	TIBA	600	5.93	20.1	16.6	135.0
14 ^{d)}	TIBA	300	8.43	29.8	13.5	135.2
15 ^{e)}	TIBA	300	6.00	24.4	17.7	134.8

^{a)}Polymerization conditions: 5 μmol of Cr, 100 mL of toluene, 50 °C, 1 bar of ethylene, 30 min, 400 rpm; ^{b)}Determined by gel permeation chromatography (GPC);

^{c)}Determined by differential scanning calorimetry (DSC); ^{d)}Reaction time: 15 min; ^{e)} Reaction time: 60 min.

Table 4. Copolymerization of ethylene and propylene by Ti-MOFs.

Entry	Precatalyst	Turnover frequency (TOF) ^{a)}	Second scan percent crystallinity (X_c) ^{b)}	T_M ^{b)}	% propylene ^{c)}
1	Ti(III)-MFU-4l	3806	37%	125	4 ± 1%
2	Ti(IV)-MFU-4l	126	38%	127	6.7 ± 1.3%

^{a)}Reported as moles of ethylene consumed per mole of exchanged metal per hour; ^{b)}Evaluated by differential scanning calorimetry (DSC); ^{c)}Determined by solid-state nuclear magnetic resonance (NMR). Conditions: ethylene (10 bar), propylene (9 bar), and MAO in toluene (23 °C, 1 h).

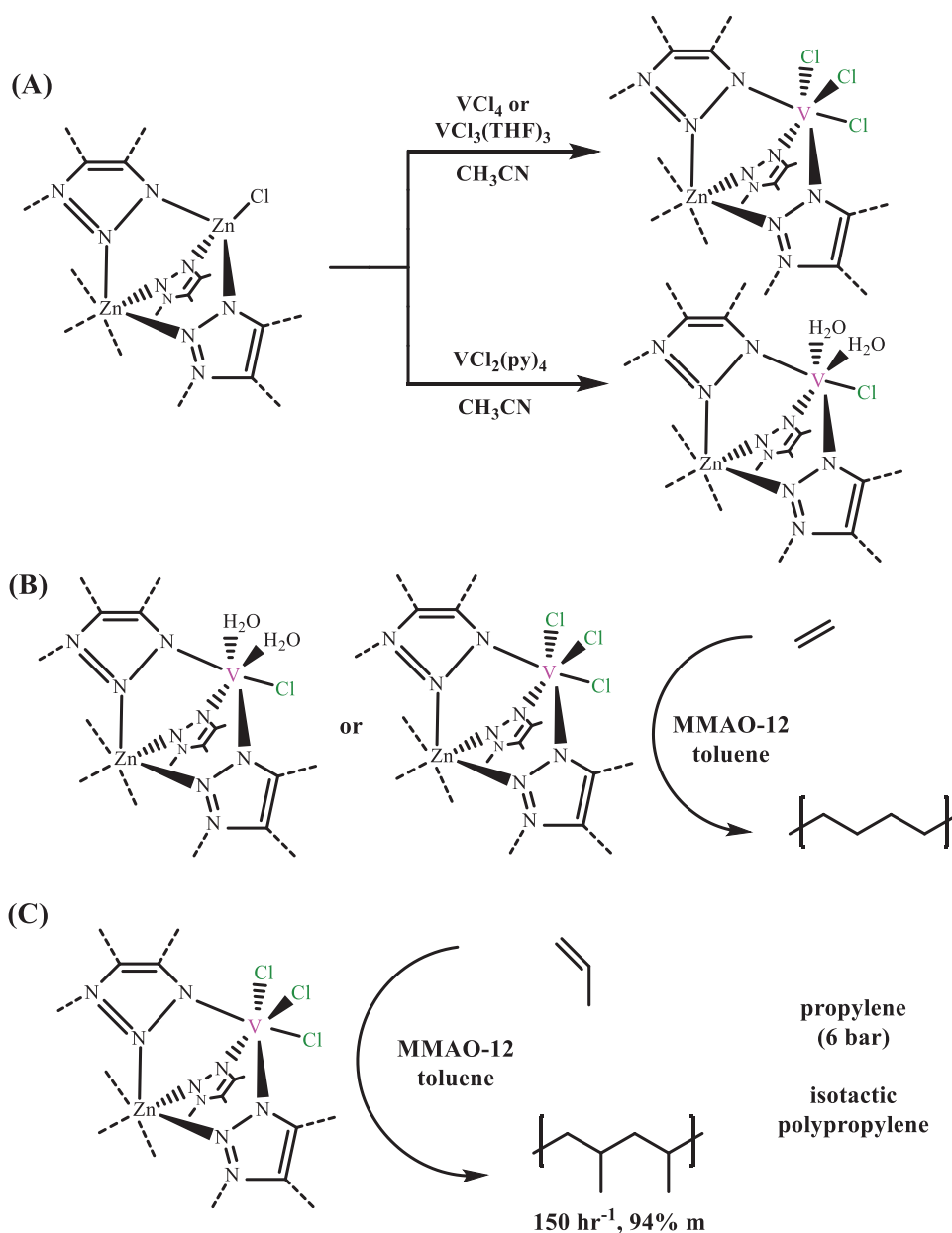


Figure 12. V(II)-MFU-4l and V(IV)-MFU-4l A) for ethylene B) and propylene C) polymerization with the activation of (modified methylaluminoxane) MMAO-12.

could be used in 24 h polymerization without any loss of activity.

5. Late Transition Metal-Based MOFs

Bulky steric hindrance substituents in late transition metal catalysts (Figure 1E–G) can effectively inhibit the β -H elimination as the shielding on the axial position of metal centers.^[98–100] Faster rate of chain growth than chain transfer results in high MW (co)polymers. However, Ni-based MOFs are mainly applied for olefin oligomerization due to the lack of large steric hindrance group around the Ni(II) sites in the microenvironment. Other late transition metal based MOFs, such as Co-based MOFs used for olefin polymerization and Fe-based MOF for olefin oligomerization, have been also reported.

In addition, the nuclear charge number of late transition metals in the microenvironment is generally more than that of early transition metals, which allows late transition metal sites to bind tightly with β -H, and thus facilitating the β -H elimination for the production of various oligomers. However, the low attraction of early transition metals to β -H is beneficial for the growth of polymer chains for the production of high MW polymers.

5.1. Nickel-Based MOFs

α -Olefins (e.g., C₄, C₆, and C₈, etc.) are important raw materials for chemical industry (e.g., plastics, lubricants, etc.).^[101–103] Ni-based MOFs are highly selective and active for olefin oligomerizations and can be reused without significant loss of activities in some cases.

5.1.1. Metal Sites in the Inorganic Nodes

The modulation of metal content in the microenvironment could improve the catalytic activity of MOF catalysts. In order to reduce the preparation cost of MOF catalysts, Dincă and co-workers^[104] synthesized Ni-CFA-1 by incorporating Ni(II) ions into the inorganic nodes of Zn₅(OAc)₄(Bibta)₃ (CFA-1, OAc = acetic acid, Bibta = 1*H*,1'*H*-5,5-bibenzo[*d*][1,2,3] triazole) by cation exchange. At 50 bar ethylene pressure and 22 °C, the activity of Ni(7.5%)-CFA-1 (7.5 wt% Ni content) showed monotonic increasing trend (the highest activity of 1×10^6 g_{oligomers} mol_{Ni}⁻¹ h⁻¹) with the increase of MMAO-12 consumption due to the increase of the unsaturated active sites (Figure 13C). However, for the microenvironment modulation of Ni-CFA-1, the activity of Ni(1%)-CFA-1 (1 wt% Ni content) was lower than that of Ni(7.5%)-CFA-1 under the same conditions (Table 5), which was attributed to the fact that the number of metal sites in the microenvironment of Ni(1%)-CFA-1 was less than that of Ni(7.5%)-CFA-1. Inexpensive ligand 3,3'-diaminobenzidine could greatly reduce the production cost of Ni-CFA-1 and thus facilitates large-scale production, which provide a possibility for its application in the industrial production of ethylene oligomers.

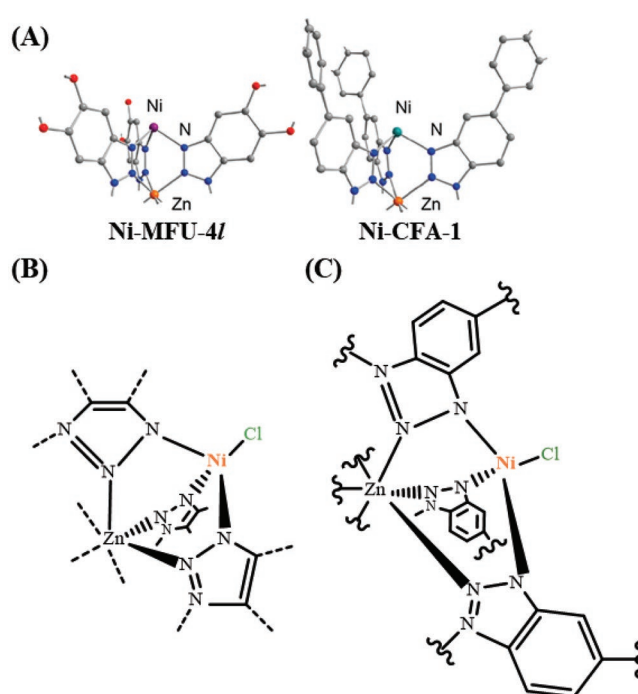


Figure 13. A) The coordination environment of Ni(II) sites within Ni-CFA-1 and Ni-MFU-4l. Reproduced with permission.^[104] Copyright 2019, American Chemical Society. B) Ni-MFU-4l and C) Ni-CFA-1 for ethylene dimerization.

Recently, Dincă and co-workers^[80] synthesized Ni-MFU-4l by incorporating Ni(II) ions into the inorganic nodes of MFU-4l by cation exchange. At 30 and 50 bar ethylene pressure, the activity and selectivity of Ni(10%)-MFU-4l (10 wt% Ni content) decreased with the increase of temperature (Table 6, entry 1–6). Elevated wt% content of Ni in Ni-MFU-4l could lead to decrease in activity due to the fact that metal agglomeration occurred

Table 5. Ni-CFA-1 for ethylene oligomerization.

Entry ^{a)}	Nickel loading	MMAO-12 equiv	TOF [h ⁻¹] ^{b)}	α -C ₄ (selectivity, wt%) ^{c)}
1	7.5%	50	13 100	93.9%
2	7.5%	100	17 900	93.2%
3	7.5%	200	29 000	90.7%
4	7.5%	250	30 600	91.3%
5	7.5%	500	31 200	96.6%
6	7.5%	1000	36 300	91.0%
7	7.5%	2000	37 100	91.2%
8	1%	100	0	—
9	1%	500	1800	87.8%
10	1%	1000	16 200	92.9%
11	1%	2000	33 300	96.6%

^{a)}As determined by gel chromatography (GC) analysis, conditions: 50 bar ethylene pressure and 22 °C; ^{b)}Moles of ethylene converted per mole of nickel per hour, determined by GC analysis; ^{c)}Percent 1-butene relative to all C₄ products.

Table 6. Ni(10%)-MFU-4l for ethylene oligomerization.

Entry	Pressure [bar]	T [°C]	MAO equiv	TOF [h ⁻¹] ^{a)}	α -C ₄ [selectivity, wt%] ^{b)}
1	50	0	100	22 600	97.8
2	50	25	100	21 000	94.6
3	50	50	100	1700	80.5
4	30	0	100	21 600	95.5
5	30	25	100	21 000	86.9
6	30	50	100	1600	83.1
7 ^{c)}	50	25	500	9100	93.0
8	50	25	500	27 000	92.3
9 ^{d)}	50	25	500	39 600	94.7
10 ^{e)}	50	25	500	41 500	94.5

^{a)} Moles of ethylene converted per mole of nickel per hour, determined by GC analysis; ^{b)} Percent 1-butene relative to all C₄ products; ^{c)} Catalyst is Ni(30%)-MFU-4l; ^{d)} Catalyst is Ni(3%) -MFU-4l; ^{e)} Catalyst is Ni(1%) -MFU-4l.

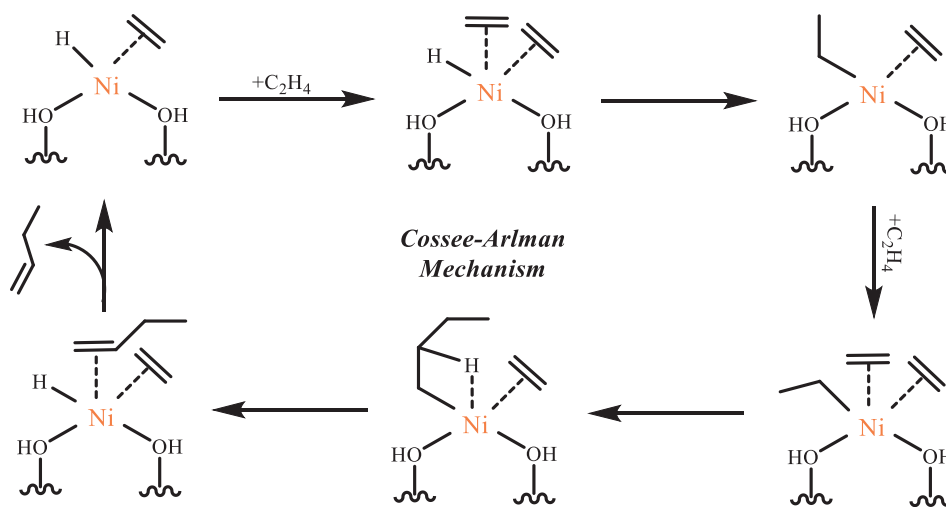
in high metal content (Table 6, entry 7–10). Ni(II) sites in Ni-MFU-4l and Ni-CFA-1 were coordinated with three N atoms (Figure 13B) in an analogous manner. However, the selectivity of Ni-CFA-1 and Ni-MFU-4l for ethylene dimerization was dissimilar due to the different microenvironment (steric hindrance) (Figure 13A) of the Ni(II) sites at 50 bar ethylene pressure.

Bhan and co-workers^[105] reported Ni-functionalized UiO-66 (Ni/UiO-66) as a stable single-site catalyst which was active for ethylene oligomerization without the activation of cocatalysts in the microenvironment for 15 days. The Cossee–Arlman steady state mechanism contributes to the understanding of ethylene oligomerization process. The Ni–H species with one ethylene molecule is adsorbed by another ethylene molecule, producing Ni–H species with two ethylene molecules. Migrating hydrogen insertion converts Ni–H species with two ethylene into Ni-ethyl species. Afterwards, another ethylene molecule coordinates with the Ni(II) sites in the Ni-ethyl species and inserts into the Ni–C(ethyl) bond to produce Ni-butyl species. The Ni-butyl species undergoes β -H elimination, generating 1-butene adsorbed

on the surface, and then the ethylene insertion for 1-butene formation (Scheme 3).

For the microenvironment modulation of Ni-UMOFNs, activation of MOF with suitable temperature allows the MOF framework to undergo partial metal oxygen/nitrogen bond breakage to achieve higher percentage of active surfaces for ethylene oligomerization. Attributed to the uniform distribution and high density of active sites in frameworks, MOFs can participate in multiple catalytic cycles. Zhang and co-workers^[77] synthesized Ni-UMOFNs-*t* with NiCl₂·6H₂O and benzene-1,4-dicarboxylate after pretreatment with different vacuum temperatures. Ni-UMOFNs-190 could be reused at least four times without significant loss of activity and selectivity (Table 7), which was attributed to the ultrathin Ni-UMOFNs-190 possessing an exceptionally high proportion of exposed active surfaces to maintain high activity after each cycle of catalytic reactions.

The application of Ni-MFU-4l to propylene oligomerization was also carried out by Dincă and co-workers.^[106] At 6 bar propylene pressure and activated by MMAO, Ni-MFU-4l exhibited the highest activity (2×10^4 g_{dimers} mol_{Ni}⁻¹ h⁻¹) for propylene



Scheme 3. The Cossee–Arlman steady state mechanism for ethylene oligomerization processes on Ni/UiO-66.

Table 7. Ni-UMOFNs-190 for ethylene dimerization.

Entry	cycle	T [°C]	Pressure [bar]	TOF [h ⁻¹]	α -C ₄ [selectivity, wt%]
1	1st	25	10	4893	72.1
2	2nd	25	10	4821	75.4
3	3rd	25	10	4571	74.1
4	4th	25	10	3929	71.4

^a) Moles of ethylene converted per mole of nickel per hour, determined by GC analysis; ^b) Percent 1-butene relative to all C₄ products.

dimerization in the form of propylene 2,1-insertion with Ni(II) sites (Figure 14). For the microenvironment modulation of Ni-MFU-4l, the regioselective 2,1-insertion might originate from the fact that the steric size of isopropyl group are greater than n-propyl group.

In contrast to the application of Ni-MFU-4l to the synthesis of propylene oligomers with branched chains by Dincă and coworkers,^[106] Mlinar and co-workers^[56] reported the application of Ni₂(dobdc) (10.3 Å) and Ni₂(dobpdc) (18.4 Å) for the production of linear propylene oligomers. At 180 °C and 5 bar propylene pressure, Ni₂(dobdc) and Ni₂(dobpdc) were active for propylene dimerization with high selectivity (>95%). Compared with MFU-4l (9.1 Å), Ni₂(dobdc) and Ni₂(dobpdc) possessing larger channels (fine microenvironment), which allows propylene to transfer easier and uniform growth of linear alkyl chains on metal-alkyl species in the channels, making it difficult for linear alkyl isomerization to occur and thus preventing the production of branched propylene dimers.

5.1.2. Metal Sites in the Organic Ligands

Two rigid ligands, 2,2'-bipyridinyl-5,5"-dicarboxylic acid and 1,1'-biphenyl-4,4"-dicarboxylic acid used to construct Ni-functionalized UiO-67-bpy (UiO-67 = [Zr₆O₄(OH)₄(BPDC)₆, BPDC = biphenyl-1,4-dicarboxylate) for ethylene oligomerization was reported by Olsbye et al.^[107] At 250 °C and 26 bar

ethylene pressure, UiO-67-bpy_{11%} (Figure 4L) with 3.1 wt% Ni content was active (1.1×10^3 g_{oligomers} mol_{Ni}⁻¹ h⁻¹) for ethylene dimerization, affording linear butene with very high selectivity (up to 99%). For the microenvironment modulation of UiO-67, the high selectivity is attributed to homogeneously distributed active sites in the microenvironment and spatial confinement, which provides strong shape selectivity for ethylene to produce products with specific structures in UiO-67.

MOFs for ethylene oligomerization are generally constructed from only one type of ligands and metals. However, Jie and co-workers^[55] performed postsynthetic modifications of MixMOFs to synthesize a series of MixMOFs-Ni (Table 8). Activated by Et₂AlCl, MixMOFs-Ni-b with 0.06 wt% Ni content was highly active (4.6×10^5 g_{oligomers} mol_{Ni}⁻¹ h⁻¹) for ethylene dimerization with high selectivity (92.7%) at 40 °C and 20 bar ethylene pressure. This is the first case for regulating the amount of Ni active sites in MOFs by varying the ratio of organic ligands possessing amino groups for the microenvironment modulation of MixMOFs-Ni, which allows binding to metal-organic complexes containing metal active centers, thus affecting the activity and selectivity of MOFs (Figure 15).

Wang and co-workers^[79] synthesized MIL-125(Ti)-NH₂-Pyr-Ni (Ni@MOF) with Ni(II) ions installed into the organic ligands of MIL-125(Ti)-NH₂-Pyr via postsynthetic modifications (Figure 16). The activity of TEA, diethyl aluminum chloride (DEAC), and ethyl aluminum dichloride (EADC)-treated Ni@MOF was greater than that of MAO-treated Ni@MOF (Table 9). For the microenvironment modulation of Ni@MOF, Ni-Cl species can be transformed into Ni-alkyl species with the activation of cocatalysts. Ni-ethyl species could be transformed to the active sites more easily than Ni-methyl species in response to ethylene stimulation, which facilitates ethylene coordination-insertion with metal sites in the microenvironment for the production of various oligomers. MIL-125(Ti)-NH₂-Pyr-Ni showed good stability and recyclability since it could be reused at least twice without any change in activity and selectivity. Moreover, the support MIL-125(Ti)-NH₂ constructed from relatively inexpensive raw materials affords new opportunities for application of MOFs in ethylene value-added processes.

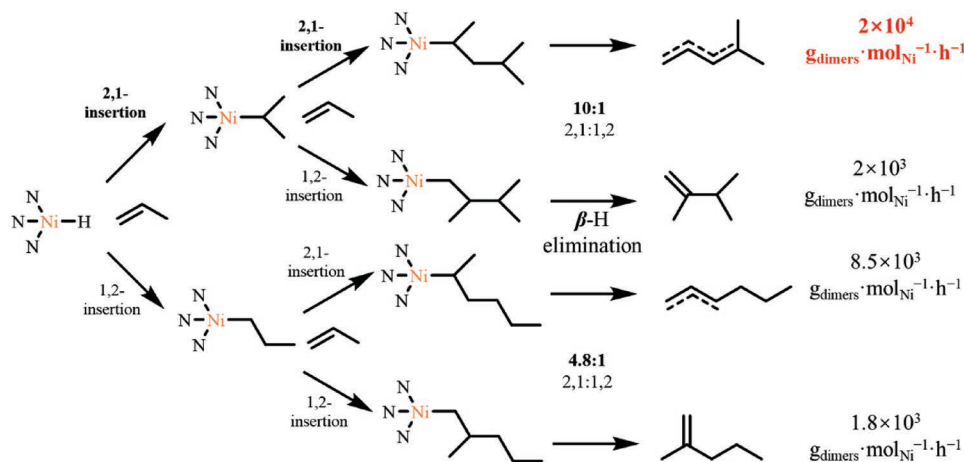


Figure 14. Single-site Ni-MFU-4l for propylene selective dimerization.

Table 8. Results of synthetic MOFs and their postsynthetic modification.

MOFs	H ₂ -aminobenzene-1,4-dicarboxylate (ABDC)/H ₂ BDC	ABDC/BDC in MixMOFs ^{a)}	Postsynthetic complexes	Ni content ^{b)} [10 ⁻³ mol g ⁻¹]
MixMOFs-a	1/5	1.85/10.15	MixMOFs-a-Ni	0.65
MixMOFs-b	1/3	2.53/9.47	MixMOFs-b-Ni	1.07
MixMOFs-c	1/2	3.43/8.57	MixMOFs-c-Ni	1.22

^{a)}Determined by ¹H NMR; ^{b)}Measured by inductively coupled plasma (ICP).

5.1.3. Metal Sites in the Channels

For microenvironment modulation, spatially confined reactions could be achieved by confining individual molecules to nanoscale spaces (e.g., MOF channels). The energy distribution of the reaction in the confined space is significantly altered, which can yield a different behavior in chemical equilibrium and kinetics than the macroscopic reaction system, thus allowing the reaction to proceed with high selectivity and activity.^[63,108]

Recently, Farha and co-workers^[50] prepared NU-1000-bpy-NiCl₂ (Figure 4L) by carrying out postsynthetic modification of NU-1000 (31 Å) with mesoporous channels. The catalyst can be applied to more than three times gas-phase ethylene oligomerizations without significant loss of activity (1.8×10^5 g_{oligomers} mol_{Ni}⁻¹ h⁻¹) and produced butylene with high selectivity (up to 95%) at room temperature (Figure 17). Whether under batch or continuous flow conditions, NU-1000-bpy-NiCl₂ was highly active for ethylene dimerization since the large channels (favorable microenvironment) of NU-1000 facilitated the transport of ethylene in MOFs and the separation of the product from the catalyst.

Canivet and co-workers^[51] synthesized Ni(10%)@(Fe)MIL-101 (10 wt% Ni content, (Fe)MIL-101 = Fe₃F(H₂O)₂O(BDC)₃) and Ni(30%)@(Fe)MIL-101 (30 wt% Ni content) with Ni(II) ions incorporated into the *N,N*-chelating centers of MOFs by postsynthetic modification. At 30 bar of ethylene pressure

and in the presence of Et₂AlCl, 10Ni@(Fe)MIL-101 (Figure 4L) showed high activity (1.8×10^5 g_{oligomers} mol_{Ni}⁻¹ h⁻¹) for ethylene dimerization, and afforded butylene with selectivity (>90%) (Figure 18). For the microenvironment modulation of Ni@(Fe)MIL-101, the BET surface of 10Ni@(Fe)MIL-101 (1110 m² g⁻¹) was larger than 30Ni@(Fe)MIL-101 (155 m² g⁻¹), which resulted in better ethylene transport and more opportunities for ethylene contact with the metal sites, making 10Ni@(Fe)MIL-101 (95%) higher selective for ethylene dimerization than 30Ni@(Fe)MIL-101 (94%).

5.2. Other Late Transition Metal-Based MOFs

Ni-based MOFs are generally applied for olefin oligomerization, while other late transition metals (e.g., Fe and Co) based MOFs are primarily used for olefin polymerization. Moreover, Fe and Co based MOFs with wide channels provide the confinement effect to retain the reactivity of the monomers.

The vacuum heating can modulate the number of active sites in the microenvironment, thus affecting the activity and selectivity of the polymerization reactions. MOFs for olefin oligomerizations are generally applied for the production of α -olefins. Interestingly, a series of MIL-100(Fe)-*t* prepared by treating Fe₃O(H₂O)2F[C₆H₃(CO₂)₃]₂-*n*H₂O (MIL-100(Fe))^[109] at different vacuum temperatures for the production of alkanes was first reported by Zhang and

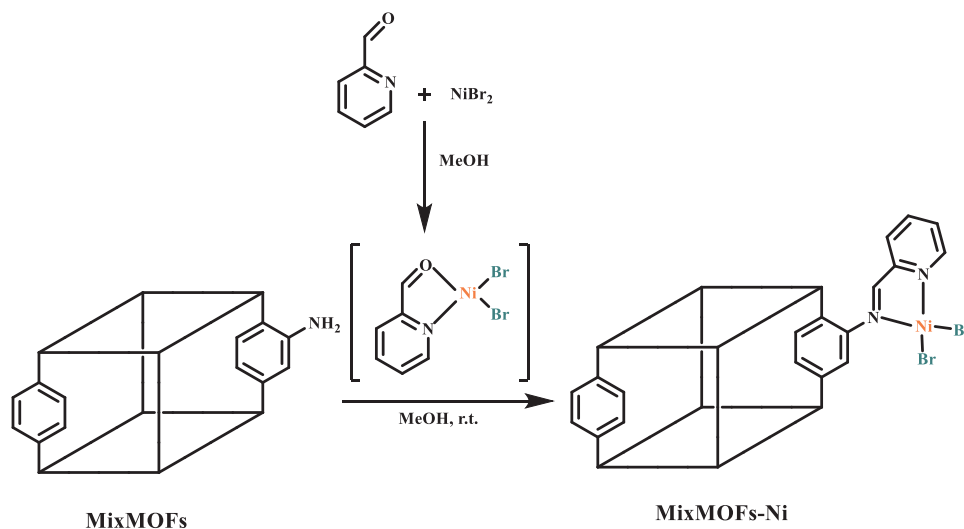


Figure 15. Preparation of MixMOFs-Ni.

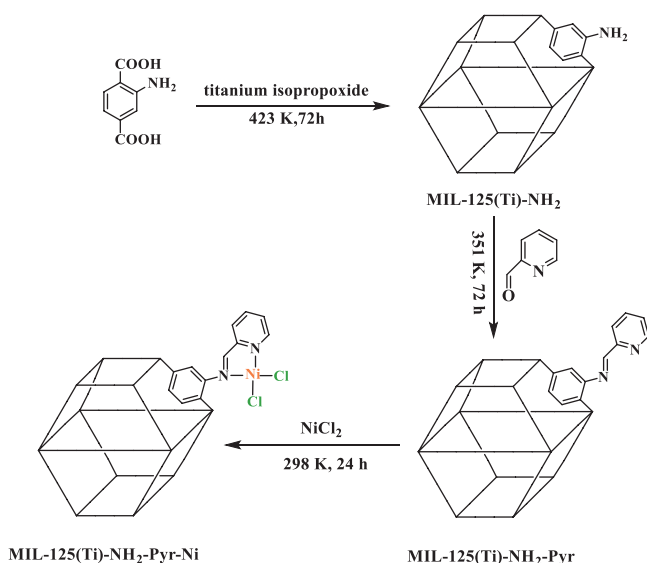


Figure 16. The flow chart for production of MIL-125(Ti)-NH₂-Pyr-Ni.

co-workers.^[70] Activated by Et₂AlCl, MIL-100(Fe)-250 showed high activity (1.2×10^5 g_{oligomers} mol_{Fe}⁻¹ h⁻¹) and very high selectivity (97.9%) for octane formation at 25 °C and 10 bar ethylene pressure. For the microenvironment modulation of MIL-100(Fe), the quantity of Fe(II) unsaturated sites in the microenvironment is increased under vacuum heating, accompanied by the reduction of Fe(III) sites (with low selectivity and activity for octane), which causes an enhancement of the selectivity and activity for octane generation.

The well-ordered channels (good microenvironment) in MOFs can be employed for the production of structure-specific polymers with desirable performances. Inspired by MOFs for mono-olefin polymerization, Dincă and co-workers^[69] initially reported Co(II)-MFU-4l prepared by installing Co(II) ions into the inorganic nodes of MFU-4l^[110] for polymerization of dienes. Activated by MMAO-12, Co(II)-MFU-4l exhibited low activity (1.4×10^4 g_{PB} mol_{Co}⁻¹ h⁻¹) for polybutadiene (PB, *cis*-1,4) formation ($M_w = 2.5 \times 10^5$) with narrow D ($D = 1.26$) and very high selectivity (99.3%) at 21 °C for 6 h (Figure 19).

Lanthanide metals based MOFs are also used as active centers in olefin polymerization. Nd-based MOFs, such as porous Nd(BTB)(H₂O)-2(C₆H₁₂O) (MIL-103(Nd), BTB = 1,3,5-benzen-

etrisbenzoate) and nonporous Nd(H₂O)(C₆H₃-(CO₂)₃) (MIL-81(Nd)), used for isoprene polymerization (Figure 20) was first reported by Visseaux et al.^[54] Activated by MMAO, porous MIL-103(Nd) was active for polyisoprene (*cis*-1,4) generation ($M_w = 3.4 \times 10^5$) with high selectivity (up to 90.7%) and narrow D ($D = 2.4$) at room temperature for 20 h. At 50 °C for 20 h, nonporous MIL-81 enabled the polymerization of isoprene, generating polyisoprene (*cis*-1,4) ($M_w = 2.0 \times 10^5$) with moderate selectivity (70.6%) and narrow D ($D = 2.6$).

6. Conclusions

MOFs possess structural diversity, channel modifiability, and uniformly-distributed metal sites in the frameworks, which could provide effective modulation of microenvironment surrounding the catalytic sites and thus have great potential to control the composition, surface area, particle size, particle size distribution, and porosity of (co)polymers, resulting in the ability to tailor the polymer properties in the heterogeneous industrial polymerization processes.

Regarding the use of MOF for olefin polymerization, it is now possible to conclude the influence of its microenvironment on the catalytic effect. For the factors of electronic effects, the presence of metal sites is the prerequisite for heterogeneous polymerization catalysis, and the microenvironmental modulation surrounding the metal sites is necessary condition for improving the catalytic performance and the properties of polymerization products. Coordination-unsaturated or coordination-saturated metal sites could be transformed to active sites by means of vacuum activation and methylation before they can be used in olefin polymerization. The tunable functional groups surrounding the metal sites provides steric hindrance to effectively inhibit β-H elimination because of its shielding effect on the axial position of the metal centers. The rate of chain growth is faster than that of chain transfer, which results in the generation of high MW (co)polymers. For the factors of spatial effects, regulation groups, the large specific surface area, total volume, and pore size would be beneficial for increasing the exposure chances of the active sites and the contact probability of olefins with the active sites to enhance the utilization of active sites and catalytic activity. In addition, we recommend that early transition metals (e.g., Zr, Cr, V, and Ti) based MOFs be designed for olefin polymerization and late transition metals (e.g., Ni and Fe) based MOFs for olefin oligomerization.

There are many methods to introduce coordination unsaturated metal sites into parent MOFs to construct active sites for olefin oligomerization and (co)polymerization. Among them, precise postsynthetic modification of the microenvironment surrounding metal centers in MOFs is an essential prerequisite for controlling polymer morphology and properties. Overall, the microenvironment refers to the electronic effects of active metals and coordination atoms, the electronic and spatial effects of surrounding regulatory groups, and the pore capacity, pore size, and specific surface area of MOFs. Not only the monomer transport rate in the channels and its opportunity to contact with metal sites, but also the activity and selectivity of

Table 9. Ni@MOF for ethylene oligomerization with the activation of cocatalysts.

Catalyst	Cocatalyst	Activity ^{a)}	α-C ₄ [wt%] ^{b)}	α-C ₆ [wt%] ^{c)}
Ni@MOF	MAO	1.81	87.2	91.5
Ni@MOF	TEA	2.07	73.9	70.2
Ni@MOF	DEAC	2.56	64.3	63.2
Ni@MOF	EADC	2.30	61.1	62.0

^{a)}Unit of 10^5 g_{oligomers} mol_{Ni}⁻¹ h⁻¹; ^{b)}Percent 1-butene relative to all C₄ products; ^{c)}Percent 1-hexene relative to all C₆ products. Conditions: 800 equiv. of cocatalyst, 50 °C, 10 bar ethylene pressure.

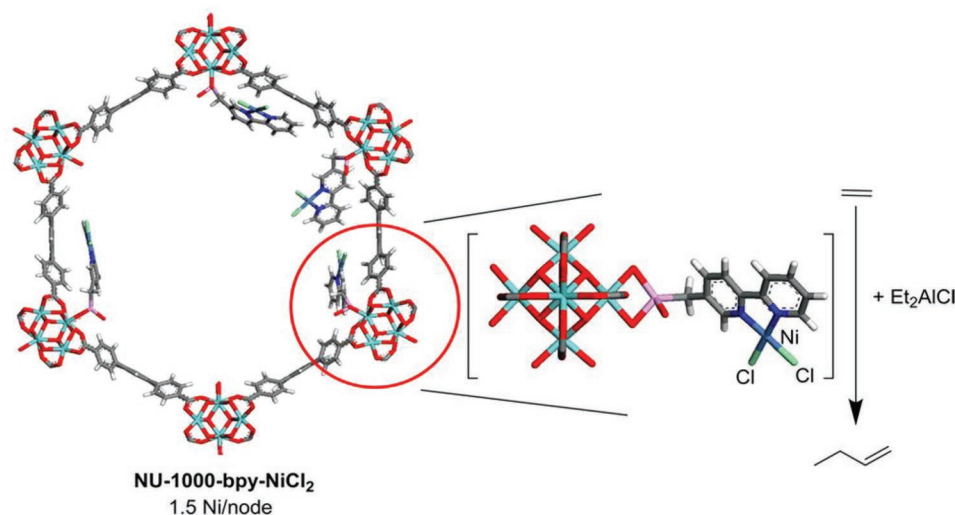


Figure 17. NU-1000-bpy-NiCl₂ for ethylene dimerization. Reproduced with permission.^[50] Copyright 2015, American Chemical Society.

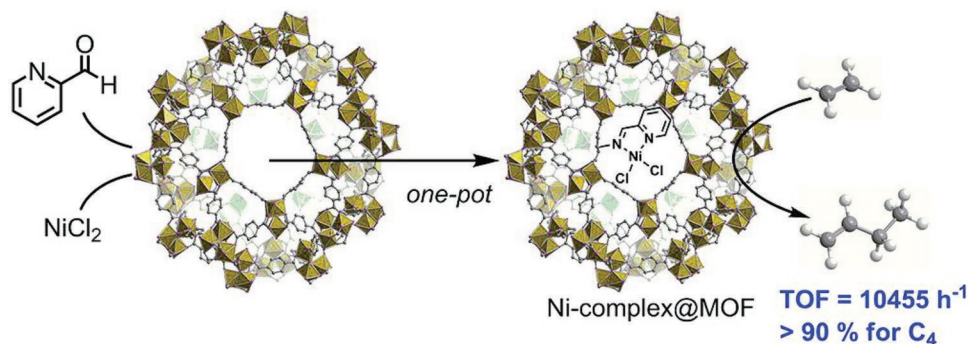


Figure 18. Ni@(Fe)MIL-101 for ethylene dimerization. Reproduced with permission.^[51] Copyright 2013, American Chemical Society.

coordination-insertion, chain growth, and chain transfer steps are crucially impacted by microenvironment modulation of MOFs.

Nevertheless, there are still some challenges for MOFs in olefins oligomerization and (co)polymerization. For instance,

the poor reusability of MOFs in olefin oligomerization, the complexed process and harsh conditions of preparation of organic ligands, the high cost of large-scale production and application of MOFs based catalysts, and the deactivation of MOFs derived from deposited polymers around the catalytic sites.

Several effective approaches could be employed to address these problems. To achieve commercial olefins polymerization with MOFs, raw materials for the preparation of MOFs should be bulk commodities (easily available and low cost) and preparation processes of MOFs are supposed to be precise, fast, and environmental under reasonable conditions. For diminished accumulation of polymer chains in the channels, it is prospective to modulate the pore size of MOFs, introduce flexible substituents around active centers and enhance the percentage of surface active sites by rational selection and design of MOFs building units. Further understanding of structure–performance relationships by computer assisted molecular simulation or machine learning would be beneficial for the design and preparation of industrial heterogeneous catalysts in the future.

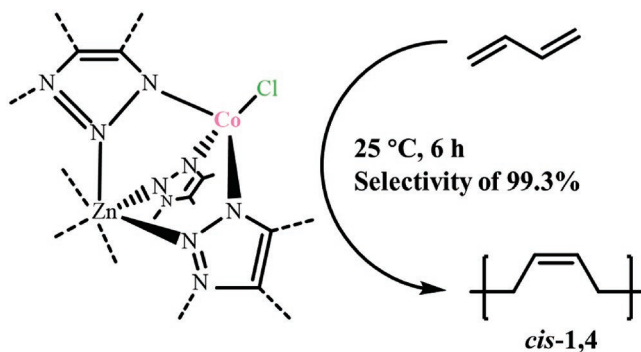


Figure 19. Highly selective Co(II)-MFU-4l for the polymerization of polybutadiene (*cis*-1,4) (>99%).

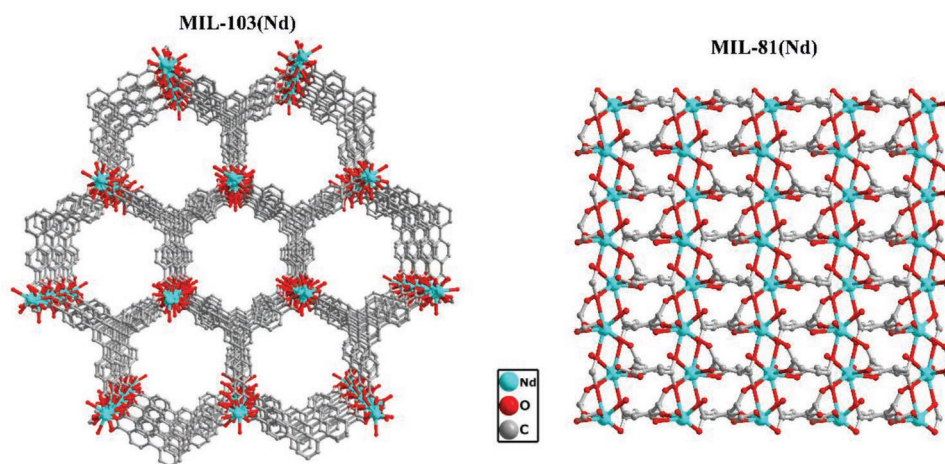


Figure 20. Porous MIL-103(Nd) and nonporous MIL-81(Nd) for the production of polyisoprene (cis-1,4).

Acknowledgements

This work was supported by grants from the National Natural Science Foundation of China (No. 22101006), Science and Technology Commission of Shanghai Municipality (No. 22QB1402800), Anhui Natural Science Foundation Youth Project (No. 1908085QB49).

Conflict of Interest

The authors declare no conflict of interest.

Keywords

coordination polymerization, metal–organic frameworks, microenvironments, oligomerization, polyolefin, transition metals

Received: September 26, 2022

Revised: November 26, 2022

Published online:

- [1] K. Ziegler, E. Holzkamp, H. Breil, H. Martin, *Angew. Chem.* **1955**, 67, 426.
- [2] G. Natta, P. Pino, P. Corradini, F. Danusso, E. Mantica, G. Mazzanti, G. Moraglio, *J. Am. Chem. Soc.* **1955**, 77, 1708.
- [3] J.-S. Wang, K. Matyjaszewski, *J. Am. Chem. Soc.* **1995**, 117, 5614.
- [4] K. Matyjaszewski, *Macromolecules* **2012**, 45, 4015.
- [5] M. Kamigaito, T. Ando, M. Sawamoto, *Chem. Rev.* **2001**, 101, 3689.
- [6] K. Min, H. Gao, K. Matyjaszewski, *J. Am. Chem. Soc.* **2005**, 127, 3825.
- [7] W. Kaminsky, D. J. Kopf, P. D. H. Sinn, H.-J. Vollmer, *Angew. Chem.* **1976**, 88, 688.
- [8] L. Resconi, L. Cavallo, A. Fait, F. Piemontesi, *Chem. Rev.* **2000**, 100, 1253.
- [9] G. W. Coates, R. M. Waymouth, *Science* **1995**, 267, 217.
- [10] E. Hauptman, R. M. Waymouth, J. W. Ziller, *J. Am. Chem. Soc.* **1995**, 117, 11586.
- [11] R. Kravchenko, A. Masood, R. M. Waymouth, C. L. Myers, *J. Am. Chem. Soc.* **1998**, 120, 2039.
- [12] L. K. Johnson, S. Mecking, M. Brookhart, *J. Am. Chem. Soc.* **1996**, 118, 267.
- [13] K. E. Allen, J. Campos, O. Daugulis, M. Brookhart, *ACS Catal.* **2015**, 5, 456.
- [14] Z. Chen, M. D. Leatherman, O. Daugulis, M. Brookhart, *J. Am. Chem. Soc.* **2017**, 139, 16013.
- [15] V. A. Kryuchkov, J.-C. Daigle, K. M. Skupov, J. P. Claverie, F. M. Winnik, *J. Am. Chem. Soc.* **2010**, 132, 15573.
- [16] J. Xia, Y. Zhang, J. Zhang, Z. Jian, *Organometallics* **2019**, 38, 1118.
- [17] B. S. Xin, N. Sato, A. Tanna, Y. Oishi, Y. Konishi, F. Shimizu, *J. Am. Chem. Soc.* **2017**, 139, 3611.
- [18] Y. Konishi, W.-j. Tao, H. Yasuda, S. Ito, Y. Oishi, H. Ohtaki, A. Tanna, T. Tayano, K. Nozaki, *ACS Macro Lett.* **2018**, 7, 213.
- [19] G. G. Hlatky, *Chem. Rev.* **2000**, 100, 1347.
- [20] G. Fink, B. Steinmetz, J. Zechlin, C. Przybyla, B. Tesche, *Chem. Rev.* **2000**, 100, 1377.
- [21] B. Jongsomjit, S. Ngamposri, P. Praserttham, *Catal. Lett.* **2005**, 100, 139.
- [22] M. Zhang, H. Xu, C. Guo, Z. Ma, J. Dong, Y. Ke, Y. Hu, *Polym. Int.* **2005**, 54, 274.
- [23] D. A. Estenoz, M. G. Chiovetta, *J. Appl. Polym. Sci.* **2001**, 81, 285.
- [24] R. Huang, D. Liu, S. Wang, B. Mao, *Macromol. Chem. Phys.* **2004**, 205, 966.
- [25] J. A. Fernandes, A.-L. Girard, in *Multimodal Polymers with Supported Catalysts*, (Eds: A. R. Albulnia, F. Prades, D. Jeremic), Springer, Cham **2019**, pp. 55–80.
- [26] B. F. Hoskins, R. Robson, *J. Am. Chem. Soc.* **1989**, 111, 5962.
- [27] S. Kitagawa, R. Kitaura, S.-I. Noro, *Angew. Chem., Int. Ed.* **2004**, 43, 2334.
- [28] G. Férey, C. Mellot-Draznieks, C. Serre, F. Millange, *Acc. Chem. Res.* **2005**, 38, 217.
- [29] N. W. Ockwig, O. Delgado-Friedrichs, M. O’Keeffe, O. M. Yaghi, *Acc. Chem. Res.* **2005**, 38, 176.
- [30] Y. Deng, B. Chi, J. Li, G. Wang, L. Zheng, X. Shi, Z. Cui, L. Du, S. Liao, K. Zang, J. Luo, Y. Hu, X. Sun, *Adv. Energy Mater.* **2019**, 9, 1802856.
- [31] J. Wang, N. Li, Y. Xu, H. Pang, *Chem. — Eur. J.* **2020**, 26, 6402.
- [32] J.-T. Liu, Y. Xie, Q. Gao, F.-H. Cao, L. Qin, Z.-Y. Wu, W. Zhang, H. Li, C.-L. Zhang, *Eur. J. Inorg. Chem.* **2020**, 2020, 581.
- [33] Y. Peng, M. Zhao, B. Chen, Z. Zhang, Y. Huang, F. Dai, Z. Lai, X. Cui, C. Tan, H. Zhang, *Adv. Mater.* **2018**, 30, 1705454.
- [34] Q. Ma, P. Yin, M. Zhao, Z. Luo, Y. Huang, Q. He, Y. Yu, Z. Liu, Z. Hu, B. Chen, H. Zhang, *Adv. Mater.* **2019**, 31, 1808249.
- [35] D. Zheng, H. Wen, X. Sun, X. Guan, J. Zhang, W. Tian, H. Feng, H. Wang, Y. Yao, *Chem. — Eur. J.* **2020**, 26, 17149.

- [36] Q. He, J. Liu, Z. Li, Q. Li, L. Xu, B. Zhang, J. Meng, Y. Wu, L. Mai, *Small* **2017**, *13*, 1701504.
- [37] L.-N. Chen, H.-Q. Li, M.-W. Yan, C.-F. Yuan, W.-W. Zhan, Y.-Q. Jiang, Z.-X. Xie, Q. Kuang, L.-S. Zheng, *Small* **2017**, *13*, 1700683.
- [38] B. Wang, J. Shang, C. Guo, J. Zhang, F. Zhu, A. Han, J. Liu, *Small* **2019**, *15*, 1804761.
- [39] X. Wang, W. Sun, Y. Tian, K. Dang, Q. Zhang, Z. Shen, S. Zhan, *Small* **2021**, *17*, 2100367.
- [40] M. Yoon, R. Srirambalaji, K. Kim, *Chem. Rev.* **2012**, *112*, 1196.
- [41] B. Liu, S. Jie, B. Li, *Prog. Chem.* **2013**, *25*, 36.
- [42] C. Xu, Y. Pan, G. Wan, H. Liu, L. Wang, H. Zhou, S.-H. Yu, H.-L. Jiang, *J. Am. Chem. Soc.* **2019**, *141*, 19110.
- [43] X. Ma, L. Wang, Q. Zhang, H.-L. Jiang, *Angew. Chem., Int. Ed.* **2019**, *58*, 12175.
- [44] Y.-N. Gong, L. Jiao, Y. Qian, C.-Y. Pan, L. Zheng, X. Cai, B. Liu, S.-H. Yu, H.-L. Jiang, *Angew. Chem., Int. Ed.* **2020**, *59*, 2705.
- [45] X. Ma, H. Liu, W. Yang, G. Mao, L. Zheng, H.-L. Jiang, *J. Am. Chem. Soc.* **2021**, *143*, 12220.
- [46] J. Li, H. Huang, W. Xue, K. Sun, X. Song, C. Wu, L. Nie, Y. Li, C. Liu, Y. Pan, H.-L. Jiang, D. Mei, C. Zhong, *Nat. Catal.* **2021**, *4*, 719.
- [47] D. J. Xiao, E. D. Bloch, J. A. Mason, W. L. Queen, M. R. Hudson, N. Planas, J. Borycz, A. L. Dzubak, P. Verma, K. Lee, F. Bonino, V. Crocellà, J. Yano, S. Bordiga, D. G. Truhlar, L. Gagliardi, C. M. Brown, J. R. Long, *Nat. Chem.* **2014**, *6*, 590.
- [48] T. Zhang, K. Manna, W. Lin, *J. Am. Chem. Soc.* **2016**, *138*, 3241.
- [49] Z. Li, N. M. Schweitzer, A. B. League, V. Bernales, A. W. Peters, A. B. Getsoian, T. C. Wang, J. T. Miller, A. Vjunov, J. L. Fulton, J. A. Lercher, C. J. Cramer, L. Gagliardi, J. T. Hupp, O. K. Farha, *J. Am. Chem. Soc.* **2016**, *138*, 1977.
- [50] S. T. Madrahimov, J. R. Gallagher, G. Zhang, Z. Meinhart, S. J. Garibay, M. Delferro, J. T. Miller, O. K. Farha, J. T. Hupp, S. T. Nguyen, *ACS Catal.* **2015**, *5*, 6713.
- [51] J. Canivet, S. Aguado, Y. Schuurman, D. Farrusseng, *J. Am. Chem. Soc.* **2013**, *135*, 4195.
- [52] P. Ji, J. B. Solomon, Z. Lin, A. M. Wilders, R. F. Jordan, W. Lin, *J. Am. Chem. Soc.* **2017**, *139*, 11325.
- [53] J. M. Tanski, P. T. Wolczanski, *Inorg. Chem.* **2001**, *40*, 2026.
- [54] M. J. Vitorino, T. Devic, M. Tromp, G. Férey, M. Visseaux, *Macromol. Chem. Phys.* **2009**, *210*, 1923.
- [55] B. Liu, S. Jie, Z. Bu, B.-G. Li, *RSC Adv.* **2014**, *4*, 62343.
- [56] A. N. Mlinar, B. K. Keitz, D. Gygi, E. D. Bloch, J. R. Long, A. T. Bell, *ACS Catal.* **2014**, *4*, 717.
- [57] B. Liu, S. Jie, Z. Bu, B.-G. Li, *J. Mol. Catal. A: Chem.* **2014**, *387*, 63.
- [58] R. C. Klet, S. Tussupbayev, J. Borycz, J. R. Gallagher, M. M. Stalzer, J. T. Miller, L. Gagliardi, J. T. Hupp, T. J. Marks, C. J. Cramer, M. Delferro, O. K. Farha, *J. Am. Chem. Soc.* **2015**, *137*, 15680.
- [59] H. Li, B. Xu, J. He, X. Liu, W. Gao, Y. Mu, *Chem. Commun.* **2015**, *51*, 16703.
- [60] Y.-S. Wei, M. Zhang, R. Zou, Q. Xu, *Chem. Rev.* **2020**, *120*, 12089.
- [61] B. V. K. J. Schmidt, *Macromol. Rapid Commun.* **2020**, *41*, 1900333.
- [62] T. A. Goetjen, J. Liu, Y. Wu, J. Sui, X. Zhang, J. T. Hupp, O. K. Farha, *Chem. Commun.* **2020**, *56*, 10409.
- [63] S. Mochizuki, T. Kitao, T. Uemura, *Chem. Commun.* **2018**, *54*, 11843.
- [64] A. Bavykina, N. Kolobov, I. S. Khan, J. A. Bau, A. Ramirez, J. Gascon, *Chem. Rev.* **2020**, *120*, 8468.
- [65] R. J. Comito, Z. Wu, G. Zhang, J. A. Lawrence III, M. D. Korzyński, J. A. Kehl, J. T. Miller, M. Dincă, *Angew. Chem., Int. Ed.* **2018**, *57*, 8135.
- [66] R. J. Comito, K. J. Fritzsching, B. J. Sundell, K. Schmidt-Rohr, M. Dincă, *J. Am. Chem. Soc.* **2016**, *138*, 10232.
- [67] H. D. Park, R. J. Comito, Z. Wu, G. Zhang, N. Ricke, C. Sun, T. Van Voorhis, J. T. Miller, Y. Román-Leshkov, M. Dincă, *ACS Catal.* **2020**, *10*, 3864.
- [68] C. A. Trickett, T. M. O. Popp, J. Su, C. Yan, J. Weisberg, A. Huq, P. Urban, J. Jiang, M. J. Kalmutzki, Q. Liu, J. Baek, M. P. Head-Gordon, G. A. Somorjai, J. A. Reimer, O. M. Yaghi, *Nat. Chem.* **2019**, *11*, 170.
- [69] R. J. C. Dubey, R. J. Comito, Z. Wu, G. Zhang, A. J. Rieth, C. H. Hendon, J. T. Miller, M. Dincă, *J. Am. Chem. Soc.* **2017**, *139*, 12664.
- [70] Y. Han, Y. Zhang, Y. Zhang, A. Cheng, Y. Hu, Z. Wang, *Appl. Catal., A* **2018**, *564*, 183.
- [71] L. Jiao, J. Wang, H.-L. Jiang, *Acc Mater. Res.* **2021**, *2*, 327.
- [72] M. F. Delley, C. S. Praveen, A. P. Borosy, F. Núñez-Zarur, A. Comas-Vives, C. Copéret, *J. Catal.* **2017**, *354*, 223.
- [73] O. Maury, G. Saggio, A. Theolier, M. Taoufik, V. Vidal, J. Thivolle-Cazat, J.-M. Basset, *C. R. Acad. Sci., Ser. IIC: Chem.* **2000**, *3*, 583.
- [74] T. Agapie, *Coord. Chem. Rev.* **2011**, *255*, 861.
- [75] M. Lamberti, M. Mazzeo, D. Pappalardo, C. Pellecchia, *Coord. Chem. Rev.* **2009**, *253*, 2082.
- [76] A. Alzamy, M. Bakiro, S. H. Ahmed, L. A. Siddig, H. L. Nguyen, *Coord. Chem. Rev.* **2022**, *462*, 214522.
- [77] Y. Hu, Y. Zhang, Y. Han, D. Sheng, D. Shan, X. Liu, A. Cheng, *ACS Appl. Nano Mater* **2019**, *2*, 136.
- [78] S. Liu, Y. Zhang, Y. Han, G. Feng, F. Gao, H. Wang, P. Qiu, *Organometallics* **2017**, *36*, 632.
- [79] L. Chen, Y. Jiang, H. Huo, J. Liu, Y. Li, C. Li, N. Zhang, J. Wang, *Appl. Catal., A* **2020**, *594*, 117457.
- [80] E. D. Metzger, C. K. Brozek, R. J. Comito, M. Dincă, *ACS Cent. Sci.* **2016**, *2*, 148.
- [81] T. A. Goetjen, J. G. Knapp, Z. H. Syed, R. A. Hackler, X. Zhang, M. Delferro, J. T. Hupp, O. K. Farha, *Catal. Sci. Technol.* **2022**, *12*, 1619.
- [82] T. A. Goetjen, X. Zhang, J. Liu, J. T. Hupp, O. K. Farha, *ACS Sustainable Chem. Eng.* **2019**, *7*, 2553.
- [83] N. Stock, S. Biswas, *Chem. Rev.* **2012**, *112*, 933.
- [84] H. Reinsch, N. Stock, *Dalton Trans.* **2017**, *46*, 8339.
- [85] L. L. Böhm, *Angew. Chem., Int. Ed.* **2003**, *42*, 5010.
- [86] K. Angermund, G. Fink, V. R. Jensen, R. Kleinschmidt, *Chem. Rev.* **2000**, *100*, 1457.
- [87] P. S. Chum, K. W. Swogger, *Prog. Polym. Sci.* **2008**, *33*, 797.
- [88] H. Makio, H. Terao, A. Iwashita, T. Fujita, *Chem. Rev.* **2011**, *111*, 2363.
- [89] P. D. Bolton, P. Mountford, *Adv. Synth. Catal.* **2005**, *347*, 355.
- [90] P. J. Wilson, A. J. Blake, M. Schröder, *Chem. Commun.* **1998**, *1007*.
- [91] H. R. Bigmore, M. A. Zuideveld, R. M. Kowalczyk, A. R. Cowley, M. Kranenburg, E. J. L. McInnes, P. Mountford, *Inorg. Chem.* **2006**, *45*, 6411.
- [92] N. Adams, H. J. Arts, P. D. Bolton, D. Cowell, S. R. Dubberley, N. Friederichs, C. M. Grant, M. Kranenburg, A. J. Sealey, B. Wang, P. J. Wilson, M. Zuideveld, A. J. Blake, M. Schröder, P. Mountford, *Organometallics* **2006**, *25*, 3888.
- [93] H. R. Bigmore, S. R. Dubberley, M. Kranenburg, S. C. Lawrence, A. J. Sealey, J. D. Selby, M. A. Zuideveld, A. R. Cowley, P. Mountford, *Chem. Commun.* **2006**, *436*.
- [94] J. P. Hogan, *J. Polym. Sci., Polym. Chem. Ed.* **1970**, *8*, 2637.
- [95] E. Schwerdtfeger, R. Buck, M. McDaniel, *Appl. Catal., A* **2012**, *423–424*, 91.
- [96] B. M. Weckhuysen, R. A. Schoonheydt, *Catal. Today* **1999**, *51*, 215.
- [97] M. Rivera-Torrente, P. D. Pletcher, M. K. Jongkind, N. Nikolopoulos, B. M. Weckhuysen, *ACS Catal.* **2019**, *9*, 3059.
- [98] G. J. P. Britovsek, M. Bruce, V. C. Gibson, B. S. Kimberley, P. J. Maddox, S. Mastroianni, S. J. McTavish, C. Redshaw, G. A. Solan, S. Strömberg, A. J. P. White, D. J. Williams, *J. Am. Chem. Soc.* **1999**, *121*, 8728.
- [99] B. L. Small, M. Brookhart, A. M. A. Bennett, *J. Am. Chem. Soc.* **1998**, *120*, 4049.

- [100] L. K. Johnson, C. M. Killian, M. Brookhart, *J. Am. Chem. Soc.* **1995**, *117*, 6414.
- [101] A. Forestière, H. Olivier-Bourbigou, L. Saussine, *Oil Gas Sci. Technol.* **2009**, *64*, 649.
- [102] G. P. Belov, P. E. Matkovsky, *Pet. Chem.* **2010**, *50*, 283.
- [103] P. W. N. M. van Leeuwen, N. D. Clément, M. J. L. Tschan, *Coord. Chem. Rev.* **2011**, *255*, 1499.
- [104] E. D. Metzger, R. J. Comito, Z. Wu, G. Zhang, R. C. Dubey, W. Xu, J. T. Miller, M. Dincă, *ACS Sustainable Chem. Eng.* **2019**, *7*, 6654.
- [105] B. Yeh, S. P. Vicchio, S. Chheda, J. Zheng, J. Schmid, L. Löbber, R. Bermejo-Deval, O. Y. Gutiérrez, J. A. Lercher, C. C. Lu, M. Neurock, R. B. Getman, L. Gagliardi, A. Bhan, *J. Am. Chem. Soc.* **2021**, *143*, 20274.
- [106] R. J. Comito, E. D. Metzger, Z. Wu, G. Zhang, C. H. Hendon, J. T. Miller, M. Dincă, *Organometallics* **2017**, *36*, 1681.
- [107] M. Kõmurcu, A. Lazzarini, G. Kaur, E. Borfecchia, S. Øien-Ødegaard, D. Gianolio, S. Bordiga, K. P. Lillerud, U. Olsbye, *Catal. Today* **2021**, *369*, 193.
- [108] C. H. Sharp, B. C. Bukowski, H. Li, E. M. Johnson, S. Ilic, A. J. Morris, D. Gersappe, R. Q. Snurr, J. R. Morris, *Chem. Soc. Rev.* **2021**, *50*, 11530.
- [109] P. Horcajada, S. Surblé, C. Serre, D.-Y. Hong, Y.-K. Seo, J.-S. Chang, J.-M. Grenèche, I. Margiolaki, G. Férey, *Chem. Commun.* **2007**, 2820.
- [110] D. Denysenko, M. Grzywa, M. Tonigold, B. Streppel, I. Krkljus, M. Hirscher, E. Mugnaioli, U. Kolb, J. Hanss, D. Volkmer, *Chem. — Eur. J.* **2011**, *17*, 1837.



Chuanlei Zhang obtained his B.S. and M.S. degrees from Hunan University of Science and Technology in 2009 and 2012, Ph.D. degree from Nanjing University in 2015. Subsequently, he started his academic career at Nanjing University and University of Science and Technology of China, respectively. Since 2015, he has been the full-time teacher at Anqing Normal University, where he currently works on Anhui UHMWPE Fiber Engineering Research Center.



Tao Zhou received his B.S. degree (2020) in materials chemistry from Anqing Normal University. He is currently a graduate student under the guidance of Prof. Chuanlei Zhang at Anqing Normal University. His research focuses on metal-covalent organic frameworks (MCOFs) for ethylene polymerization.



Yong-Qing Li was born in 1987 in Shandong, China. He received his B.S. degree in 2009 from the Hunan University of Science and Technology and M.S. degree in 2012 from the Shanghai Research Institute of Chemical Industry where he afterwards worked as an engineer. In 2021, he started his Ph.D. study at the East China University of Science and Technology under the guidance of Professor Gui-Ping Cao. His research interests are organometallic chemistry, computational chemistry, polymer chemistry, and polymerization reaction engineering.



Ye-Bin Guan obtained his M.S. degree from Anhui Normal University in 2004 and Ph.D. degree from Science and Technology of University of China in 2010. Then, he started his academic career at Anqing Normal University. Nowadays, he has been a full professor at Anhui UHMWPE Fiber Engineering Research Center.



Yu-Cai Cao was born in Hunan, China, in 1975. He received his Ph.D. degree from Zhejiang University in 2002 and then joined Shanghai Research Institute of Chemical Industry. After a post-doctoral stay at Akita University from 2004 to 2006, he started research and development of organometallic catalysis. His current status is deputy head of the State Key Laboratory of Polyolefins and Catalysis. His research is focused on olefin polymerization, high performance polyolefin materials, and synthetic organic chemistry.



Gui-Ping Cao was born in 1965. He received his Bachelor's degree in Materials Science and Engineering from East China University of Science and Technology (ECUST) in 1988, and his Master's and Doctor's degree in Chemical Engineering from ECUST in 1991 and 1997, respectively. He has been a full professor at the same university since 2001. He subsequently joined Université de Lille and North Carolina State University as a Visiting Professor from 2006 to 2007. His research interests are specialized in deep understanding of the nature relationships of "property-multiscale structure-engineering" in material science and engineering fields.